Ceramic Coatings for Metallic Interconnects and Metal Alloys Support for Solid Oxide Electrolysis Applications

Ceramic coatings for metallic interconnects and metal alloys support for solid oxide electrolysis applications

[a] E. Zanchi, [b] A.G. Sabato, [c] H. Javed, [d] A. Drewniak, [d] D. Koszelow, [d] S. Molin, [a] F. Smeacetto

[a] *Politecnico di Torino, Department of Applied Science and Technology, Corso Duca degli Abruzzi 24, 10129, Torino, Italy*

[b] *Institut de Recerca en Energia de Catalunya (IREC), Jardins de les Dones de Negre, 1, 2ª pl., 08930 Sant Adrià de Besòs, Barcelona, Spain*

[c] *Sunfire GmbH, Gasanstaltstraße 2, 01237 Dresden, Germany*

[d] *Faculty of Electronics, Telecommunications and Informatics, Gdansk University of Technology, ul. G. Narutowicza 11/12, 80-233 Gdansk, Poland*

1. Introduction

In a solid oxide electrolysis cell (SOEC) system, the metallic interconnect generally provides the electrical connection for a SOEC stack and gas separation between the cells, as well as gas distribution across the cells. Furthermore, the role of the metallic interconnect to support ceramic element layers with a low-cost and robust material, which is expected to lower the cost of solid oxide cells (SOCs) devices, has growth of interest for these materials in the field of metal-supported solid oxide electrolysis cells (MS-SOECs). Aluminium-containing alloys cannot be used as a support in MS-SOEC devices due to material requirements, since the alumina scale has too poor electrical conductivity, despite proving extremely good corrosion properties. Therefore, the best candidates for MS-SOEC applications seems to be chromia forming ferritic alloys (**Shaigan et al. 2010**).

Stainless steels are widely considered as the most promising candidates as state of the art interconnect materials due to their electrically-conducting oxide scale and an appropriate ~~coefficient of~~ thermal expansion coefficient (~~CTE~~TEC). Specifically, chromia-forming stainless steels are commonly used as interconnect materials because of ~~CTE~~ TEC matching with adjacent materials, low cost and good formability.

A good oxidation resistance is provided by the formation of a continuous Cr_2O_3-scale with a relatively slow Cr diffusion and an acceptable electronic conductivity at the operating temperatures (**Quadakkers et al. 2003**).

Formatted: Heading 1, Left, Numbered + Level: 1 + Numbering Style: 1, 2, 3, … + Start at: 1 + Alignment: Left + Aligned at: 0.63 cm + Indent at: 1.27 cm

Commented [ML1]: To be consistent with other chapters

The deposition of specific ceramic protective coatings onto the interconnects has been demonstrated as an effective method to limit the degradation issues and to increase the lifetime of the SOEC stack by lowering the corrosion rate and blocking the chromium evaporation.

There is a growing body of literature that recognises the importance of ceramic coatings as key materials in determining the durability and performance of SOEC stacks. An effective coating for SOEC metallic interconnect must specifically fulfil the following requirements:

- Reduce the oxidation rate of the steel substrate by limiting the oxygen inward diffusion as well as the Cr outward diffusion
- Limit the Cr evaporation rate and the consequent electrodes poisoning
- Ensure high electrical conductivity to minimise the ohmic losses
- Good thermo-chemical stability with respect to the other stack components
- Good thermo-mechanical compatibility with the steel substrate

Enhanced efficiency of SOEC stacks can be reached only by appropriate material choice with good performance and functional requirements. In addition to a high electrical conductivity, another key requirement for the coating is their TEC, which should match the stainless steel, in order to avoid spallation or delamination phenomena.

The spinel family has attracted great attention as reliable coating materials; some of the spinel compositions investigated are: Co-Mn, Cu-Mn, Cu-Fe, Mn-Fe, Ni-Fe. To date, several studies have shown that the Co-Mn spinel family has demonstrated the best performances in terms of functional requirements and properties; the existing literature on Mn-Co spinel is extensive and focuses particularly on deposition methods, tests in relevant conditions etc.

Modified Mn-Co based spinels have started attracting significant attention as alternative compositions, and recent studies dive further into the feasibility of using different spinel compositions.

The first section of the subchapter is focused on the proposed solutions as ceramic coatings and their compositional and functional modifications, describing the most common deposition methods, the influence on their chemical composition and the corrosion and the electrical behaviour in relevant conditions during long term test assessment.

The results that are presented here will show how spinel coatings play a key role in the interconnect performance, while pointing out some unanswered questions about their functional properties and some future perspectives for additional research.

The first part of this section will examine different materials proposed as coatings for interconnects, starting from reactive elements oxides, rare earth perovskites to spinels.

The second part deals mainly with different methods of modification of the Mn-Co spinel composition, specifically focusing on the effect of Cu and Fe addition and describing the optimization of the coating processing by the electrophoretic co-deposition method. Most of the techniques related to the modifications of Mn-Co based material by electrophoretic co-deposition methods are critically presented, and the new horizons that are opening up, to improve the performances of spinel coatings for SOEC interconnects application, are discussed.

This subsection will also discuss how the implementation of electrophoresis technique can offer innovative solutions when adapted with other slurry-based deposition techniques (i. e. dip coating or electrolytic deposition) and perspectives for an industrial upscale of the electrophoretic deposition technique.

The second section of this subchapter is concerned with an overview of porous metal alloys and their relevant role as metal-supported solid oxide electrolysis cells (MS-SOECs), from methods of production, moving to their corrosion properties and potential innovative tests to assess their interface stability, i. e. with glass-based sealings.

The conclusion section presents and summarizes the findings of some specific aspect of this research, focusing on the two key themes that have been reviewed and discussed, thus making some recommendations for future research work and progress on durability issues of solid oxide electrolysis cells devices

Materials

Different protective coatings and deposition techniques have been developed in the recent years in order to limit the Cr-poisoning and an excessive oxide scale growth.

The characteristics of each material used as protective coating has to be considered also in relation with the properties of the metallic substrate under the points of view of possible chemical interactions (especially with Cr) and coefficient of thermal expansion. In Table 1, the most used ferritic stainless steels up to now are summarized with their Cr content and their TEC.

The protective materials typically used today for this application can be classified in three main categories: reactive elements oxides, rare earth perovskites and spinel-based, as shown in Table 2, where an overview of the main properties is given.

Table 1: Cr content and TEC of common ferritic stainless steels used as interconnect for SOC stacks(**Thyssenkrupp 2001a**; **Thyssenkrupp 2001b**; **VDM-Metals 2010**; **ThyssenKrupp VDM GmbH 2012**).

Steel	Cr (wt.%)	~~CTE~~ TEC (10^{-6} K^{-1})
Crofer22APU	22	12.6
Crofer22H	22	12.3
AISI430	16.5	12
AISI441	18	10.5

Table 2: classification and properties of materials for protective coatings (**Mah, Muchtar, Somalu, and Ghazali 2017**).

Coating material	Electronic conductivity	Cr migration inhibition	Oxidation rate reduction	Simplicity of deposition
Reactive elements oxide	Fair	Poor	Good	Good
Rare earth perovskites	Good	Fair	Poor	Fair
Spinels	Good	Good	Fair	Good

Reactive element oxides (REO)

In the past, the effect of deposition of reactive elements (i.e. Y, La, Ce, etc.) oxides (REO) or their combination on the surface of chromia forming stainless steels have been widely investigated (**Hou 2000**; **Qi and Lees 2000**; **Chevalier and Larpin 2002**). The presence of these elements ~~have~~has been demonstrated to be effective in improving the adhesion of the oxide scale to the steel and to limit its oxidation, thus reducing the area specific resistance (ASR) which is directly related to the oxide scale thickness. Many studies reported the deposition of these materials on metallic interconnects for ~~solid oxide cells~~SOC applications (**Qu et al. 2004**; **Fontana et al. 2007**; **Piccardo et al. 2007**; **Shaigan et al. 2010**; **Fontana et al. 2012**; **Mah, Muchtar, Somalu, and Ghazali 2017**). Fontana et al. (**Fontana et al. 2012**) demonstrated the effectiveness of La_2O_3 and Y_2O_3 deposition on Crofer22APU in oxidising atmosphere up to more than 23kh at 800°C in air. In Figure 1~~Figure 1~~, it is possible to

Formatted: Font: Not Italic, Font color: Auto

see how the application of this REO coatings sensibly reduced the oxidation of the underlying steel even during a significant aging (30 months) especially in the case of La_2O_3.

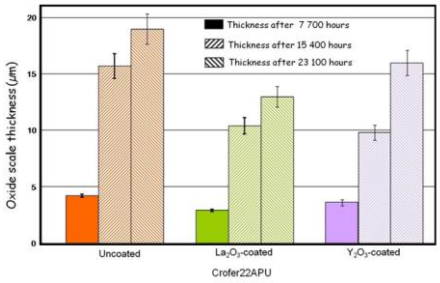

Figure 1: oxide scale thickness measured after different aging period in air at 800°C for uncoated Crofer22APU, La_2O_3 coated Crofer22APU and Y_2O_3 coated Crofer22APU. Reproduced from (**Fontana et al. 2012**).

REO coatings are generally very thin (< 1µm) and for this reason, despite their excellent effect on the oxidation, they are considered not to be effective in limiting the Cr evaporation. Indeed, in recent years the trend has been to couple reactive elements layer with Co, to reduce the Cr evaporation. In this sense, the group of Jan Froitzheim and co-workers extensively studied the application of Ce/Co coatings on different stainless steels for SOC application, investigating the effects of these coatings on ASR and Cr evaporation in different relevant conditions (**Magrasó et al. 2015**; **Falk-Windisch et al. 2017**; **Goebel et al. 2020**; **Goebel et al. 2021**). Moreover, C. Goebel et al. (**Goebel et al. 2020**) recently conducted a very extended study in which Ce/Co coatings were applied to AISI 441 and their performances were investigated in oxidising atmosphere at 800 °C up to 36 kh (4 years). In Figure 2, the results in terms of ASR and Cr evaporation are reported. The application of Ce/Co was strongly effective under both points of view in comparison with uncoated AISI 441. The Cr evaporation resulted to be at least one order of magnitude lower in comparison with the uncoated steel while the ASR resulted to be 34 mΩ cm^2 after the long aging, well below what is considered the limit value after 40 kh of aging (100 mΩ cm^2) (**Steele and Heinzel 2001**). They recently reported also the self-healing effect of these coatings when exposed at 750 °C; the self-healing was effective after only 71 h of exposition at this temperature (**Goebel et al. 2021**).

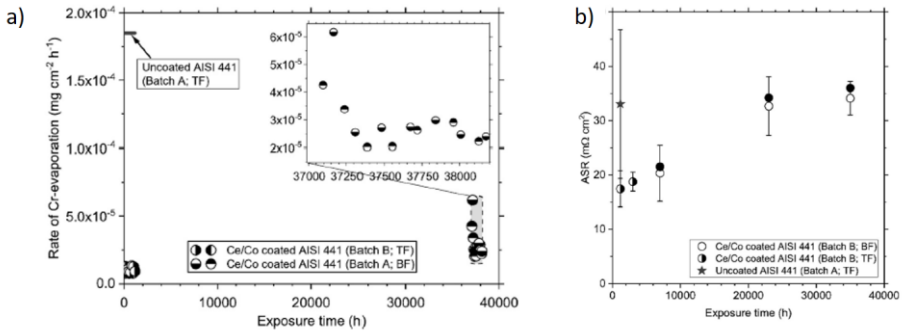

Figure 2: long term performances of Ce/Co coated AISI441 stainless steel in terms of Cr-evaporation retention (a) and ASR (b). Reproduced from (**Goebel et al. 2020**)*.*

Rare earth perovskites

Perovskites are widely used in solid oxide cells technology, typically as cathode materials. Perovskites are characterized by ABO_3 structure with the A site occupied by a trivalent cation (i.e. La) while B is occupied by a transition metal (i.e. Cr, Co, Fe, Mn etc.). In oxidising atmosphere and at high temperatures, these perovskites show p-type electronic conductivity. This, in addition to their TEC (see *Table 3: TEC of typical rare earth perovskites used as protective coatings for solid oxide cells metallic interconnects* (**Tan et al. 2019**).Table 3), makes these materials potentially suitable to act as protective coatings for the metallic interconnects. Furthermore, it is possible to modify the doping in order to tune their conductivity or TEC. Indeed, it is possible to dope the A site with large radii divalent cations (i.e. Sr, Ca) and B site with electron acceptors (i.e. Ni, Fe, Cu).

The main perovskites investigated up to now as protective layer are based on: lanthanum chromates ($LaCrO_3$) (**Johnson et al. 2004**; **Zhu et al. 2004**; **Shaigan et al. 2008**; **Jeong et al. 2020**), Sr doped lanthanum chromate ($La_{1-x}Sr_xCrO_3$) (**Belogolovsky et al. 2007**; **Paknahad et al. 2014**), lanthanum strontium manganite ($La_{1-x}Sr_xMnO_3$) (**Chu et al. 2009**; **Pyo et al. 2011**) cobaltite ($La_{1-x}Sr_xCoO_3$) (**Zhu et al. 2004**; **Persson et al. 2012**) or ferrite ($La_{1-x}Sr_xFeO_3$) (**S. Lee et al. 2010**; **Tsai et al. 2010**).

Despite their good conductivity in general, perovskite-based coatings demonstrated poor densification ability. This does not provide a sufficient barrier against Cr evaporation and thus against cathode poisoning (**Shaigan et al. 2010**; **Mah, Muchtar, Somalu, and Ghazali 2017**; **Tan et al. 2019**).

Table 3: TEC of typical rare earth perovskites used as protective coatings for solid oxide cells metallic interconnects (**Tan et al. 2019**).

Material	CTE (10^{-6} k^{-1})
LSM ($La_{1-x}Sr_xMnO_3$)	12.5
LSCF ($La_{1-x}Sr_xCo_{1-x}Fe_xO3$)	15.4
SSCF ($Sm_{1-x}Sr_xCo_{1-x}Fe_xO_3$)	16
BSCF ($Ba_{1-x}Sr_xCo_{1-x}Fe_xO_3$)	16.6
LSCM ($La_{1-x}Sr_xCo_{1-x}Mn_xO_3$)	12.5
LSCN ($La_{1-x}Sr_xCo_{1-x}Ni_xO_3$)	14.6

Spinels

In the recent years, the attention of the scientific community has been more focused on the development of spinel-based materials as protective coatings for metallic interconnects. Indeed, these materials demonstrated superior performances in comparison with both reactive elements oxides and rare earth perovskites, in terms of ASR and densification (Cr-retention ability). In addition, the spinel composition can be modified by proper doping, in order to slightly modify the properties of the coating (see next section "Modification of the spinel composition").

Different binary spinels were considered for this application with different cations in the A and B sites of the spinel generic formula AB_2O_4 in order to reach the suitable values of conductivity and ~~C~~TEC (**Shaigan et al. 2010**; **Mah, Muchtar, Somalu, and Ghazali 2017**; **Tan et al. 2019**; **Zhu et al. 2021**). The main investigated systems are reported in Table 4~~Table 4~~ with the corresponding values of ~~C~~TEC and electrical conductivity. These values can vary in a range depending from the specific composition of the spinel, synthesis and sintering methods as well as operating temperature.

Formatted: Font: Not Italic, Font color: Auto

Table 4: ~~C~~TEC and electrical conductivity values at high temperatures of typical spinel systems used as protective coatings for SOC applications (**Shaigan et al. 2010**; **Mah, Muchtar, Somalu, and Ghazali 2017**; **Tan et al. 2019**; **Zhu et al. 2021**).

Spinel system	~~C~~TEC (10^{-6} K^{-1})	σ (S cm^{-1})
Mn-Co	7.4-14	21-157
Cu-Fe	11.2	2.3-9.1

Ni-Fe	11.7-12.1	0.05-15~~.~~
Cu-Mn	11-12.6	51-100

In the case of Mn-Co based spinels, a wide range of compositions ($A_xB_{3-x}O_4$ with 1<x<2) have been investigated and resulted to be suitable as protective material (**Chesson and Zhu 2020**), in terms of ASR and Cr-retention ability even after very long aging at high T in air. Among the different considered spinels, the ones resulted more suitable for typical SOC applications were Mn_2CoO_4, $MnCo_2O_4$ and their combination (**Zhu et al. 2021**).

Smeacetto et al. (**Smeacetto et al. 2015**; **Molin et al. 2017**; **Sabato et al. 2021**) extensively studied these protective coatings, especially deposited by the electrophoretic deposition (EPD) method and tested for long aging periods (> 2000 h) in air at operating temperatures (750-850 °C). In Figure 3~~Figure 3~~ and Figure 4~~Figure 4~~, two relevant results are reported. $Mn_{1.5}Co_{1.5}O_4$ coatings demonstrated excellent performances in terms of ASR (Figure 3~~Figure 3~~) up to 2500 h at 800 °C, in comparison with uncoated Crofer22APU. The overall ASR value after 2500 h of aging at 800 °C in air resulted to be ≈20 mΩ·cm^2 versus the one of uncoated sample of ≈30 mΩ·cm^2. In addition, the degradation rate in case of bare Crofer22APU is much higher (≈5.3 mΩ.cm^2/kh) in comparison with the coated Crofer22APU (≈0.51 mΩ.cm^2/kh). In Figure 4~~Figure 4~~, it possible to observe the Cr retaining effect of the protective layer after 3000 h stack test at 850 °C. Energy dispersive X-ray spectroscopy (~~EDX~~ EDS) maps did not detected relevant Cr outward diffusion from the steel substrate to the coating during this period. Furthermore, the Cr_2O_3 oxide scale appears to be ~~≈~~2 µm thick after the aging, thus highlighting the effect of the spinel coating on limiting its growth (in accordance with a low ASR).

Formatted: Font: Not Italic, Font color: Auto

Formatted: Font: Not Italic, Font color: Auto

Formatted: Font: Not Italic, Font color: Auto

Formatted: Font: Not Italic, Font color: Auto

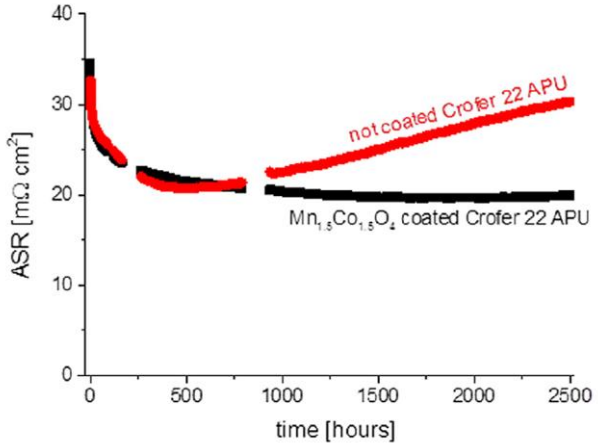

Figure 3: ASR of Crofer22APU bare and coated with $Mn_{1.5}Co_{1.5}O_4$ in air at 800 °C for 2500 h. Reproduced from (**Smeacetto et al. 2015**).

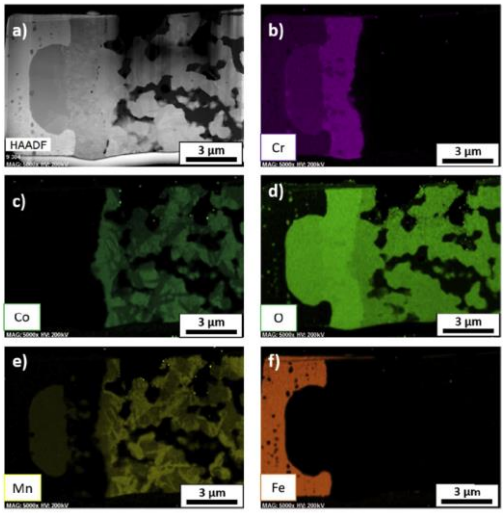

Figure 4: EDS elemental mapping of a thin lamella collected at the interface Crofer22APU/$Mn_{1.5}Co_{1.5}O_4$ after an aging of 3000 h in air at 800 °C. Reproduced from (**Sabato et al. 2021**).

Mn-Co spinels can be produced in tetragonal structure (Mn_2CoO_4) or in cubic structure ($MnCo_2O_4$), depending on the relative amount of Mn and Co. The tetragonal phase is not stable at the SOEC operating conditions, as it undergoes a tetragonal-to-cubic phase transformation around 450-600 °C. Different compositions of Mn-Co spinel were investigated with different Mn/Co ratio trying to clarify the effect of compositional changes on the electrical conductivity and TEC; a mixture of the tetragonal and cubic phase (referred with the formula $Mn_{1.5}Co_{1.5}O_4$) can be used. Concerning the electrical conductivity, a strong discrepancy is reported in literature with very different values ranging from 20 to more than 100 S cm^{-1} at 800°C (**Zhu et al. 2021**). This is related not only to the specific composition of the spinel (Mn/Co) but also to the powder synthesis and to the sintering treatment as well. Despite this huge range, all these values are considered more than enough for a protective coating since is commonly accepted that the mayor contribution to the resistance of the interconnects is given by Cr_2O_3 ($\sigma \sim 0.01$ S cm^{-1}) growth and formation of resistive reaction products with the coatings (**Goebel et al. 2018**). A recent study by Chesson et al. (**Chesson and Zhu 2020**) gave a significant contribution to this topic clarifying the properties of different Mn-Co spinels with different compositions. Their results (summarized in Figure 5) showed that with the increasing content of Mn, both the TEC and the conductivity decrease. For this reason, a suitable compromise for SOC application can be identified in intermediate compositions ($Mn_xCo_{3-x}O_4$, with $1.2<x<1.5$).

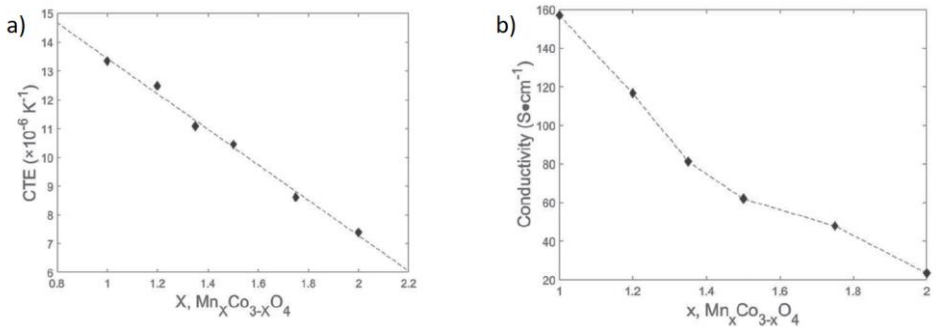

Figure 5: variation of TEC (a) and conductivity (b) in Mn-Co spinel systems with different Mn and Co content. Reproduced from (**Chesson and Zhu 2020**).

The application of Mn-Co spinel based coatings on chromia forming ferritic stainless steel often lead to the formation of a $(Mn,Co,Cr)_2O_3$ reaction layer at the interface with the Cr_2O_3 scale due to

interdiffusion of elements (**Magdefrau et al. 2013**; **Gambino et al. 2015**; **Talic et al. 2019**). A schematic mechanism is reported in Figure 6 together with a schematization of the different layers and the corresponding equivalent circuit. Due to the lower conductivity (σ ≈ 0.05 S cm^{-1}) of this reaction layer in comparison to the coating itself and excessive growth of this reaction layer can have a detrimental effect on the ASR of the system. The thickness of the reaction layer is directly related to the sintering treatment of the coatings and to the oxygen diffusion, it is crucial to have a good densification of the protective coating also to limit this phenomenon. However, the main contribution to the resistance is still represented by the Cr_2O_3 which has a conductivity of ~ 0.01 S cm^{-1}, which is five times lower than the typical conductivity reported for the reaction layer (**Zhu et al. 2021**).

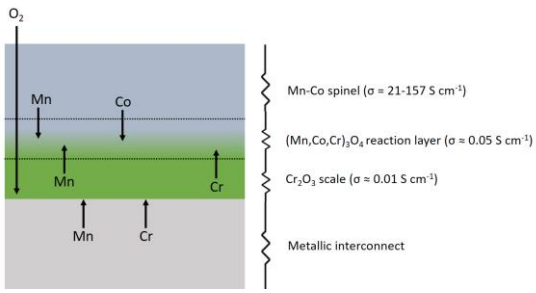

Figure 6: schematization of interdiffusion of elements at the interface of a chromia-forming stainless steel coated with Mn-Co spinel in oxidising atmosphere at high temperatures.

In recent years, also different Co-free spinels have been investigated as well, since Co is considered a critical raw material for energy applications. In particular, spinels based on the systems Ni-Fe (**P. F. You et al. 2018**; **Chesson and Zhu 2020**; **P. You et al. 2020**), Cu-Fe (**Pan et al. 2021a**; **Pan et al. 2021b**) and Mn-Cu (**Waluyo et al. 2014**; **Hosseini et al. 2015**; **Spotorno et al. 2015**; **Sun et al. 2018**; **Wang et al. 2018**) have attracted more attention. Among these the Mn-Cu spinel-based coatings have been extensively studied with promising results (Figure 7). Despite this, there is still a lack in the evaluation of their behaviour (mass gain, ASR, reactions, cathode poisoning) for long aging periods (>1000h).

Commented [ML2]: Nickel is also a CRM now…. But I think we can leave as it is.

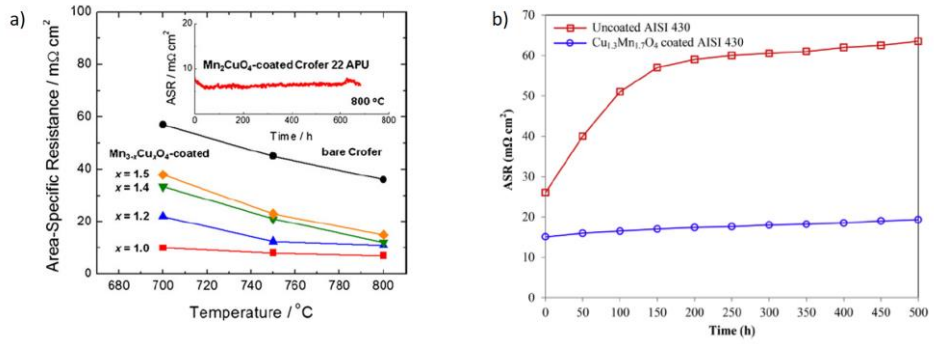

Figure 7: ASR performance of Mn-Cu spinel protective coatings on Crofer22APU (a) and AISI430 (b). Reproduced from (**Waluyo et al. 2014**) *and* (**Hosseini et al. 2015**).

Modification of the spinel composition

The Mn-Co spinel structure can accommodate a wide range of different cations: the position occupied by each cation in the spinel lattice defines the degree of distortion of the crystal structure, with major effects on the functional properties of the spinel. For these reasons, performing modification of the composition of the Mn-Co base spinel has been identified as a promising route to improve the functional properties of the base spinel structure. This spinel coating modification is normally referred as "doping" and can be achieved either by substitution of part of Mn or Co of the base spinel or by simple addition, depending on the synthesis method. Modifications of the Mn-Co spinel composition have been focused on doping by transition metals such as Cu, Fe, Ni, Ag or rare earth elements, such as Y, La, Ce.

The effect of the variation of the functional properties of the spinel depends on the specific doping element, as well as on its amount; however, doping the spinel structure does not generally cause the formation of new crystalline structures. Indeed, the doping element is accommodated in the spinel structure replacing either Co or Mn in the tetrahedral or octahedral sites; this substitution causes a distortion of the crystalline lattice.

To this purpose, doping by addition of transition elements is reported to bring a significant impact on the electrical conductivity and on the coefficient of thermal expansion. Results found in literature generally present a relevant scattering of properties, due to different experimental set-up and testing conditions. However, most of the studies focuses on doping by copper or iron.

There is general accordance on Cu increasing both electrical conductivity and TEC of the Mn-Co spinel. The reason found is the stabilization of the cubic spinel

structure lead by copper addition. Indeed, the base Mn-Co spinel exhibits a tetragonal-cubic transition that depends on the specific Mn to Co ratio in the composition; the highest electrical conductivity is achieved by increasing the cobalt content ($MnCo_2O_4$ spinel with a full cubic structure) (**Brylewski et al. 2014**). When copper is introduced in the spinel, even higher conductivity values have been reported; moreover, copper addition also leads to an enhanced sinterability, allowing to reduce sintering time and temperature to obtain satisfactory densification levels (**Masi et al. 2016**; **Mah, Muchtar, Somalu, Ghazali, et al. 2017**; **Masi et al. 2017**). Following these considerations, together with the fact that cobalt is a critical raw material, the implementation of cobalt-free Mn-Cu spinel coatings is recently gaining a lot of attention in research. However, compared to the Mn-Co spinel, the stability range of the Mn-Cu spinel is significantly narrower, meaning that CuO tends to segregate and that higher sintering temperature are needed to obtain densification suitable for application as a protective coating. For these reasons, still few studies focuses on Mn-Cu spinel coatings and further research needs to assess their protective properties (**Ignaczak et al. 2020**).

On the other hand, iron addition to the Mn-Co spinel has an opposite effect on the mentioned properties compared to copper. Indeed, Fe addition is responsible for increasing the lattice parameter of the Mn-Co spinel cubic structure resulting in lower electrical conductivity due to the lower possibility of polaron hopping (**Liu et al. 2013**; **Talic, Hendriksen, et al. 2018**). Similarly, the lower electrical conductivity is associated with a decrease in the TEC with increasing Fe content in the spinel (**Masi et al. 2016**). Regarding the spinel densification, Fe addition is reported to have small influence or to partially reduce the sinterability of the coating; results reported in literature do not fully agree due to different synthesis, deposition and sintering methods. However, the major influence of iron addition lays on the improvement of the oxidation resistance, represented by the development of a thinner oxide scale during aging. Indeed, it is apparent that Fe presence in the coating layer next to the oxide scale partially reduces the diffusion rate of chromium (**Zanchi et al. 2019**; **Zanchi et al. 2020**). Figure 8 compares coating morphology of the unmodified spinel coating (MC) with the Fe-doped (MCFe) and Cu-doped (MCCu) coatings, highlighting the different residual porosity degree (**Talic et al. 2017**).

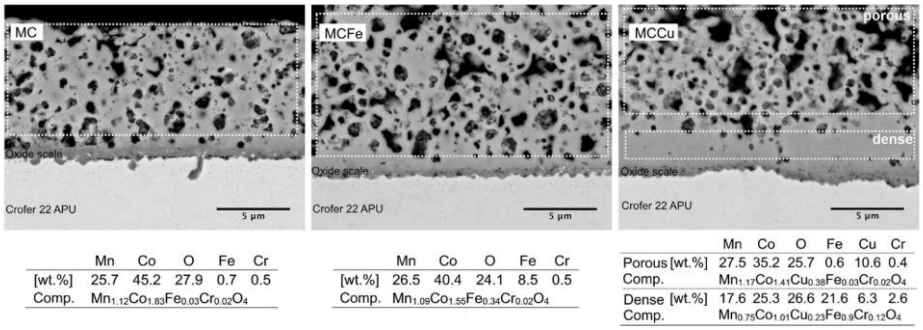

	Mn	Co	O	Fe	Cr
[wt.%]	25.7	45.2	27.9	0.7	0.5
Comp.	$Mn_{1.12}Co_{1.83}Fe_{0.03}Cr_{0.02}O_4$				

	Mn	Co	O	Fe	Cr
[wt.%]	26.5	40.4	24.1	8.5	0.5
Comp.	$Mn_{1.09}Co_{1.55}Fe_{0.34}Cr_{0.02}O_4$				

	Mn	Co	O	Fe	Cu	Cr
Porous [wt.%]	27.5	35.2	25.7	0.6	10.6	0.4
Comp.	$Mn_{1.17}Co_{1.41}Cu_{0.38}Fe_{0.03}Cr_{0.02}O_4$					
Dense [wt.%]	17.6	25.3	26.6	21.6	6.3	2.6
Comp.	$Mn_{0.75}Co_{1.01}Cu_{0.23}Fe_{0.9}Cr_{0.12}O_4$					

Figure 8: SEM backscatter images of unmodified (MC), Fe-doped (MCFe) and Cu-doped (MCCu) spinel coatings on Crofer22APU. Reproduced from (**Talic et al. 2017**).

A high degree of densification is essential to guarantee satisfactory protection properties of the coating, in order to limit oxygen inward diffusion to the steel interconnect (**Bobruk et al. 2018**; **Zanchi et al. 2021**). However, coating densification depends not only on the coating composition, but also on the deposition method. To this purpose, various deposition techniques can be exploited to deposit copper or iron doped Mn-Co based coatings. Dense Cu-doped coatings have been obtained by high-energy micro-arc alloying using targets of metallic alloys produced by argon arc melting; however, many hours of oxidation are required to form homogeneous oxide layers with this technique (**P. Guo et al. 2018**; **P. Y. Guo et al. 2020**). Also highly dense Fe-doped spinel coating have been produced by atmospheric plasma spray, but thermal decomposition of the spinel was encountered during deposition from the target (**Puranen et al. 2014**). In general, majority of the studies focuses on slurry-based deposition methods. Dip coating followed by two-step sintering of Cu-doped manganese cobalt spinel synthetized by citric acid nitrate process is quite reported in literature (**B. K. Park et al. 2013**; **Chen et al. 2015**; **Xiao et al. 2016**; **Li et al. 2017**); on the other hand, slurry painting followed by repeated stages of infiltration and sintering has been used for Fe-doped spinels previously synthetized by sol-gel method (**Molin et al. 2016**). An innovative deposition technique is represented by the ink-jet printing from water-based inks of iron-modified spinel; despite the good potential of the technique, the performance of the obtained coatings still need to be assessed (**Pandiyan et al. 2020**).

Apart from copper and iron, fewer studies have been focused on Ni- and Ag doped Mn-Co spinel. Although available results are limited, nickel is suggested to improve the electrical conductivity and sinterability compared to the unmodified spinel, but by a lower degree than copper (**B. K. Park et al. 2013**). Doping with silver can significantly increase the electrical conductivity of the Mn-Co spinel; however the long term stability of the coating, as well as the sustainability of using a

precious metal in a large scale production of the SOC device still need to be assessed (**K. Lee et al. 2017**).

As anticipated in the previous section, rare earth elements can reduce the steel oxidation rate and favour better adhesion of the oxide scale (**Hou and Stringer 1995**; **Seo et al. 2008**; **Hassan et al. 2020**). In recent years, some studies have demonstrated that rare earth elements can be employed to modify the Mn-Co spinel. For example, lanthanum-doped Mn-Co spinel have been produced by high-energy micro-arc alloying (HEMAA) process using targets obtained by argon arc melting (**P. Guo et al. 2018**; **P. Y. Guo et al. 2020**). Similarly, La- and Ce- doped Mn-Co spinel coatings have been deposited by magnetron sputtering from commercial sputter targets consisting of the doped spinels: in this case, doping with lanthanum was proved to be strongly effective in reducing oxidation rate and chromium vaporization from the steel substrate in comparison with the unmodified spinel and Ce-doping as well (**Tseng et al. 2020**). A Ce-doped Mn-Co synthesized by glycine-nitrate combustion synthesis method and deposited by screen printing on AISI 441 showed similar behaviour than the un-doped Mn-Co spinel coating in the study of Stevenson et al. (**Stevenson et al. 2013**). The possible application of Y-doped Mn-Co spinel processed by sol-gel method have been investigated by Xin at al. (**Xin et al. 2011**): the modified coating applied through a spinel powder reduction coating technique expressed satisfactory properties as protective coating. More recently, a Cu-Y-doped Mn-Co spinel obtained by glycine nitrate process has been proposed: the coating was deposited by screen printing and demonstrated promising behaviour with reference to the uncoated steel substrate, but no comparison with performance of the unmodified coating is provided in the study (**Thaheem et al. 2021**).

Optimization of the coating deposition by electrophoretic co-deposition method

As reviewed in the previous paragraph, the doped spinels have been synthetized before coating deposition: spray pyrolysis, citric acid nitrate process, Pechini method and solid state reaction are some of the synthesis techniques reported in literature. After the synthesis, doped spinels have been deposited through dip coating, slurry painting, screen and inkjet printing, plasma spray and magnetron sputtering. Other studies focused on the use of high-energy micro-arc alloying (HEMAA) technique to deposit from targets of modified metallic alloys obtained from argon arc melting. All the mentioned techniques require multi-step processes, involving first the spinel synthesis or the metallic alloy preparation and then the coating deposition and can be grouped as “ex-situ” spinel modification routes.

Electrophoretic deposition allows to deposit well adherent layers of ceramic particles in few seconds and by means of a simple and adaptable set-up. Thanks to the versatility for materials employed and coatings morphology, as well as the low-energy demand, EPD is considered a suitable technique for industrial applications in SOC technology (**Kalinina and Pikalova 2021**; **Zhu et al. 2021**).

Electrophoretic deposition of base spinel was first proposed in 2015 as a viable and effective deposition technique for SOC metallic interconnect coatings (**Smeacetto et al. 2015**), then followed by numerous studies highlighting the advantages of EPD in reducing processing time and cost of the interconnect (**Zanchi et al. 2021**). Talic et al. (**Talic et al. 2017**) have demonstrated the feasibility to process Cu or Fe modified Mn-Co spinel with controlled amount of doping elements via spray pyrolysis from aqueous based nitrate solutions; the obtained powders have been successfully deposited by electrophoretic deposition using a fully organic solvent mixture. More recently, commercial Cu-Mn-Co commercial powder was deposited by EPD and various organic solvent media were compared (**Aznam et al. 2021**). In both cases, the green layers were stabilised by a two-step sintering, consisting of a reduction treatment followed by a re-oxidation: indeed, this approach is generally accepted as the optimal post-deposition treatment to densify protective spinel coatings. Furthermore, some attempts must be made to optimize the sintering procedure, toward faster and cheaper methods. For example, Javed et al. (**Javed et al. 2021**) have proposed an innovative sintering procedure involving the use of pressure assisted flash sintering, requiring just few minutes to obtain highly densified Mn-Co spinel coating.

Field Code Changed

Field Code Changed

EPD of base and modified spinel powders has already demonstrated promising results, in terms of both processing and performances of the coatings and it is now raising interest thanks to the possibility of obtaining doped spinel coatings by a co-deposition method. This upgrade of the technique allows to modify the coating composition “in-situ”, i.e. during the deposition process, reducing processing time and cost compared to ex-situ synthesis methods.

This process does not require any modification of the deposition set-up or instrument configuration compared to the electrophoretic deposition of a single element; however, special attention must be paid to the preparation of the EPD suspension and choice of deposition parameters.

Indeed, the first and simplest kinetic model of electrophoretic deposition proposed by Hamaker in 1940 correlates the deposited mass m [g] to the concentration Cs [g cm^{-3}] and the mobility μ [cm^2 s^{-1} V^{-1}] of the solid particles, the electric field E [V cm^{-1}], the deposition area S [cm^2] and deposition time t [s] through the following equation (**Hamaker 1940**):

$$m = C_s \, \mu \, E \, S \, t$$

However, when a co-deposition is performed the reported formula can result further complicated by the addition of factors for each material inserted in the suspension. Moreover, parameters regarding the mutual interaction between the different colloidal particles used should be considered as well. Indeed, the deposition kinetic can significantly vary depending on the material employed and the possibility of deposit single powders alone is no guarantee of success of the co-deposition process.

On practical level, the following parameters must be taken into consideration when optimising a suspension for the electrophoretic co-deposition process:

- Selection of the powders; as for electrophoresis of single element, selected powders to co-deposit must have a suitable particle size distribution and develop a surface charge high enough to avoid flocculation and sedimentation. Although there is not a general cut-off value of particle size for electrophoretic deposition, the diameter of employed powders is commonly < 1 µm. Moreover, in the case of co-deposition, it is important to consider interactions between the different particles
- Formulation of the suspension: the powders to co-deposit must be all stable (not decompose) in the solvent or the mixture of liquid media selected for the suspension. Moreover, the environmental impact of the liquid medium must be considered, giving priority to water-based solutions. When a stable suspension cannot be reached, making use of stabilizers or dispersant agents is necessary.
- Post-deposition treatment: electrophoretic deposition allows to deposit well packed layers of particles; however, performing a post-deposition sintering treatment is always necessary in order to stabilize and densify the green coating and to achieve good protective performances. When electrophoretic co-deposition is performed, the optimised sintering profile usually foresees two subsequential thermal treatments. A first treatment in reducing atmosphere (a mixture of Ar/H_2 or N/H_2) ensures a partial reduction of Mn-Co spinel in metallic Co and MnO; in the case or iron doping, Fe_2O_3 is also reduced, forming an intermetallic Co-Fe compound. The subsequent heat treatment is performed in air and leads to the re-oxidation of the reduced coating, with the formation of the final spinel structure. Depending on the doping element, the spinel structure can stabilise either the cubic or the tetragonal crystalline phase. In the case of iron doping, the cubic phase is partially stabilized, together with a distortion of the lattice (**Zanchi et al. 2019**): as shown in Figure 9, the degree of lattice distortion depends on the amount of Fe addition to the spinel

and it is visible as a shift of the diffraction peak toward lower 2Theta angles. Cu doping is reported to stabilize the cubic phase without lattice distortion appreciable by XRD analysis.

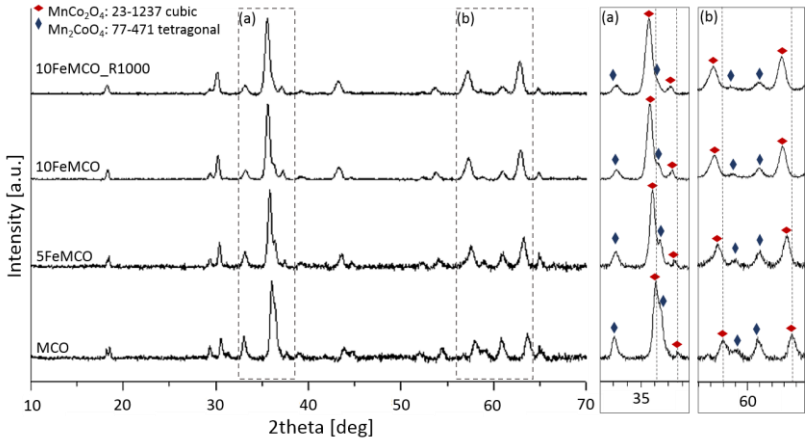

Figure 9: X-Ray diffraction patterns of as-sintered Fe-doped manganese-cobalt spinel coatings, reproduced form (**Zanchi et al. 2019**). *The diffraction pattern of the unmodified $Mn_{1.5}Co_{1.5}O_4$ (MCO) is compared with those of $Mn_{1,43}Co_{1,43}Fe_{0,14}O_4$ (5FeMCO) and $Mn_{1,35}Co_{1,35}Fe_{0,30}O_4$ (10FeMCO).*

Up to now, the electrophoretic co-deposition technique has been successfully exploited to produce Cu-doped (**Molin et al. 2018**; **Sabato et al. 2019**) and Fe-doped Mn-Co spinel coatings (**Zanchi et al. 2019**; **Zanchi et al. 2020**). Coating processing approach as well as the evaluation of performances at SOC relevant conditions are reviewed and discussed in the following section. As schematically represented in Figure 10, the electrophoretic deposition mechanism through which Cu or Fe doping has been performed is opposite, although both the same suspension and deposition parameters have been employed. Indeed, in the case of Cu doping, zeta potential measurements proved both coating precursors developed a positive surface charge in the suspension: +13 mV for $Mn_{1.5}Co_{1.5}O_4$ and +6 mV for CuO. Despite the lower surface charge developed by CuO, deposition performed at 50V for 30s was effective to co-deposit both precursors preserving their relative amount in the EPD suspension in the deposited coating as well. On the other hand, Fe_2O_3 develops a negative zeta potential of -10 mV; however, a fully cathodic co-deposition is preserved up to 10 wt.% addition of iron oxide to the $Mn_{1.5}Co_{1.5}O_4$ suspension. Indeed, the electrostatic interactions between opposite charges and the smaller dimension of the iron precursor in comparison to Mn-Co spinel resulted in the deposition mechanism reported in the figure.

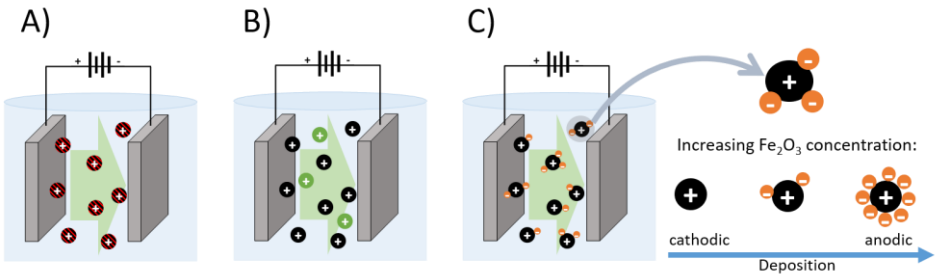

Figure 10: Schematic diagram showing the electrophoretic deposition process of manganese-cobalt spinel-based coatings. A) ex-situ doped spinel; B) in-situ copper doping; C) in-situ iron doping. Reproduced form (**Zanchi et al. 2021**).

Coatings obtained by electrophoretic co-deposition were processed and tested at slightly different conditions, allowing to reveal properties brought by various addition of Cu or Fe.

Both Cu- and Fe-doped coatings were sintered by two-step treatment, with reducing and re-oxidising steps performed at 900 °C. Moreover, only Fe-doped coatings were reduced also at 1000 °C, to evaluate whether the higher sintering temperature could improve the sinterability of the spinel.

Copper doping lead to great densification, as clearly visible in Figure 11. The residual porosity was found to be dependent on both the amount of copper addition and oxidation time due to a continuous sintering effect. However, coatings obtained with the highest doping level (labelled as 10CuMCO in Figure 11) underwent pores coalescence during 3000 h aging at 800 °C: this effect can be detrimental for protection properties as it can facilitate cracks propagation and suggests that a lower amount of copper addition would be favourable.

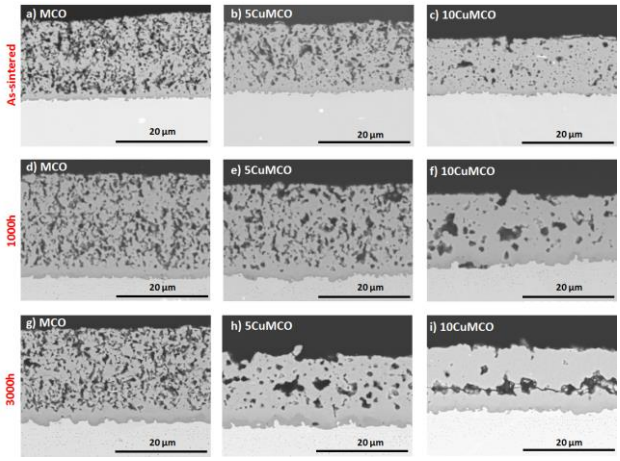

Figure 11: Cross section SEM images of the coated samples after different aging periods: as-sintered (a, b and c), after 1000h (d, e and f) and after 3000h (g, h and i) reproduced from (**Sabato et al. 2019**)*. The picture compares the densification level of undoped coating (MCO) and Cu-doped coatings (5CuMCO and 10CuMCO) with aging time.*

In terms of oxidation resistance and area specific resistance measured at 800 °C on Crofer 22 APU substrate, Cu-doped Mn-Co coatings demonstrated similar results than the undoped spinel; indeed, as suggested by the review of previously published works, doping seems to have smaller influence on coatings properties at highest working temperature, due to more sever oxidation phenomena (**Zanchi et al. 2021**). To this purpose, Fe-doped coatings tested at 750 °C, expressed clearer trends depending on doping level, as visible from oxidation resistance test results reported in Figure 12 (**Zanchi et al. 2019**). Indeed, despite similar values of residual porosity, iron addition was proved to significantly reduce the growth rate of the oxide scale compared to the base spinel coating (MCO), bringing beneficial effects on the oxidation rate. Furthermore, Fe-doped coatings reduced at higher temperature (named 10FeMCO_R1000) exhibited slightly better densification, which resulted essential to limit the degree of internal oxidation and obtain the best performances.

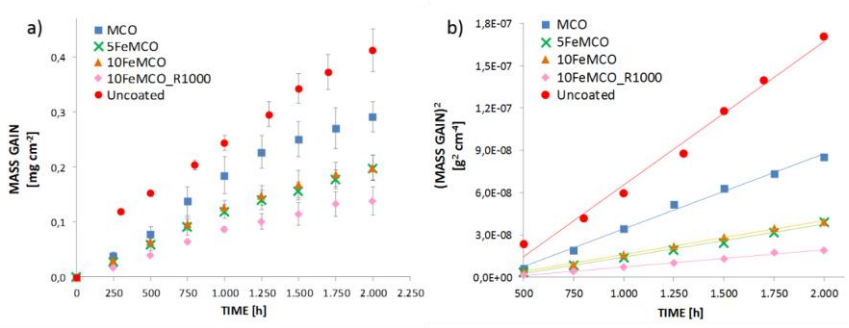

Figure 12: (a) Mass gain and (b) Parabolic rate plot of coated and bare Crofer22APU during cyclic oxidation at 750 °C in air, 2000 h. Reproduced from (**Zanchi et al. 2019**).

Conductivity measurements performed on sintered pellets confirmed higher resistivity for Fe-doped spinel at higher temperatures as well as thermal activated electronic conduction, in agreement with the results reported in various studies (**Masi et al. 2016**; **Talic, Hendriksen, et al. 2018**). Results are reported in Figure 13. However, areas specific resistance test monitored for more than 3000 h at 750°C for both Crofer22APU and AISI 441 coated steel revealed that the composition of the alloy substrate has a major influence on defining the degradation mechanism and the performance of the interconnect (**Zanchi et al. 2020**). Indeed, the minor presence of residual impurities in the cheaper AISI 441 alloy is believed to modify diffusion mechanisms with benefits for coating densification and conductivity of the oxide scale.

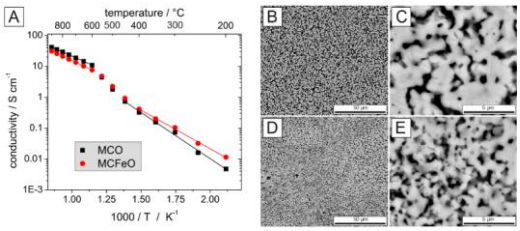

Figure 13: Results of electrical conductivity measurements (A) and microscopy images of samples microstructure: B,C) Unmodified spinel (MCO); D,E) Fe-doped Mn-Co spinel (MCFeO).

The discussion on the influence of the steel substrate results even more relevant considering the current attempts in progressively reducing the operating temperature of SOC stacks. This effort will open to the possibility of using cheaper alloys as interconnect, but also to the need of developing more efficient coatings to prolong the stack working life. To this purpose, optimising the coating deposition method through electrophoretic co-deposition could allow to modify in-house coating

composition and properties, acting on EPD suspension precursors and sintering treatment, depending on the requirement of the stack.

Discussed results on Cu and Fe spinel doping set the groundwork for future research on the implementation of spinel composition. Considering the better sinterability and higher conductivity of the Cu-doped Mn-Co spinel, as well as the improvement of oxidation resistance related to Fe-doping, it is proposed that a simultaneous Cu-Fe doping of the base Mn-Co spinel is viable approach to improve the performance of the coating. A search of the literature revealed a lack of a comprehensive evaluation in this direction, despite the already suggested possibility of tuning spinel functional properties by Fe and Cu doping into the Mn-Co spinel (**Masi et al. 2016**). In this framework, the electrophoretic co-deposition plays a key role.

Apart from co-deposition, the implementation of electrophoresis technique can offer innovative solutions when adjusted with other slurry-based deposition techniques such as dip coating or electrolytic deposition (ELD), in order to produce multilayer or composite coatings as suggested by few recent publications.

For example, a hybrid ELD-EPD approach has been proposed to produce CeO_2 composite spinel coatings with the aim of coupling the benefits of rare earth addition with those of Mn-Co spinel coating. Firstly, Zhu et al. (**Zhu et al. 2015**) prepared coatings from electrolyte solution of cobalt salts, to which Mn_3O_4 and CeO_2 powders were added; a CeO_2-$(Co,Mn)_3O_4$ composite coating was obtained after thermal conversion treatment at 600-800 °C for a total of 10 h. More recently, Mosavi et al. (**Mosavi and Ebrahimifar 2020**) worked on electrolyte solution containing manganese sulphate and cobalt sulphate with further addition of CeO_2 powders deposited on AISI 430 substrate. After oxidation of 200 h, $MnCo_2O_4$ and CeO_2 phases were detected; however, the formation of $MnFe_2O_4$ spinel due to relevant diffusion of iron from the steel substrate defines the need of further investigations on the long-term stability of the coating.

Furthermore, Brylewski et al. (**Brylewski et al. 2021**) have reported on a multilayer system consisting of a coating of gadolinium oxide obtained by dip coating followed by EPD of $MnCo_2O_4$. Dip coating allows to deposit a thin layer of the rare earth oxide on the steel surface, where it is more effective in reducing the oxide scale growth by segregation at the steel grain boundaries; coupled with the spinel coating, this innovative approach provided improved protection at 800 °C.

A natural progression of this work is to analyse the possibility to upscale to industrial relevant size of the coating deposition technique. Indeed, all the studies and deposition methods mentioned in the previous paragraphs are related to the deposition and test of protective coatings on small lab-

scale samples of few square centimetres. However, real-size interconnects can present larger dimensions (some hundreds of square centimetres) as well as corrugated and channelled surfaces. To this purpose, the investigation on feasibility and sustainability for the industrial application is a fundamental requirement for the validation of the proposed deposition technique. For example Blum et al. (**Blum et al. 2020**) have recently reported a study on long-term stack test including metallic interconnects coated by atmospheric plasma spray and wet powder spray (**Bianco et al. 2019**). Similarly, atmospheric plasma spray coating is mentioned in the study of Menzler et al. (**Menzler et al. 2018**) on post-test characterization of 30 000 h stack operation; on the other hand, Bianco et al. (**Bianco et al. 2019**) studied the degradation of a stack with interconnect coated by wet powder spray. In all the few mentioned publications, authors have never focused on the evaluation of the coating deposition technique on the stack performance. To this purpose, electrophoretic deposition has been validated as a valuable deposition technique to scale up to industrial relevant conditions (**Sabato et al. 2021**). The study proved the feasibility to adapt the EPD set-up to coat 20 x 20 cm^2 steel interconnect, including complex shapes and channelled surfaces; furthermore, the stack test performed for 3000 h at 850 °C confirmed excellent performances of the coating, setting a significant step forward in the use of EPD as versatile, low cost, easy and reproducible method in the solid oxide technology.

3. Porous metal alloys support in solid oxide electrolysis cells

In the last decade, advanced alloys have been discovered to be an interesting material in a variety of applications such as engines, turbines, and supercritical reactors (**M. Park et al. 2018**; **Talic, Molin, et al. 2018**; **Bianco et al. 2020**). However, the most noticeable growth of interest for these materials was in the field of metal-supported solid oxide electrolysis cells (MS-SOECs) (**Tucker 2020**). For this particular application, a lot of specific material requirements have to be fulfilled. First of all, the new material should be relatively cheap and easy to manufacture into complex shapes because the typically used SOEC interconnectors are ceramic components, which are expensive and hard to produce into specific shapes. Furthermore, the material should be able to withstand very large thermal shocks (> 100 °C/cm (**Tucker 2020**)) and extremely fast thermal cycling as SOEC support. Moreover, the main role of the SOEC interconnector is to collect a charge and transport it to the electrodes. Therefore, the support material has to have high electronic conductivity.

Taking all of the conditions into account, the best material appears to be chromia forming ferritic stainless steel. It has high enough thermal conductivity and resistance to rapid thermal shock and is cheaper than the ceramic components that are used in commercial SOEC systems. The biggest problem with applying alloys as support in MS-SOEC is the corrosion process at operating conditions. This process causes oxidation of the alloy, which significantly decreases the electrical conductivity of the support and interconnector. In spite of the fact that Al_2O_3 has very high corrosion resistance, it is also an insulator, so alumina forming alloys cannot be used as interconnectors in SOECs. However, among metal oxides, chromia (Cr_2O_3) has one of the highest electrical conductivity (~1 – 10 mS cm^{-1} at 600 – 800 °C (**Holt and Kofstad 1994**)) thus, it seems to be the best candidate for interconnector in SOEC systems.

In order to even decrease more the cost and weight of the whole device, the porous form of chromia forming stainless steel is being considered as an alternative for heavy ceramic components. The basic difference between dense and porous alloys is their specific surface area (SSA), and for the alloy of ~30 % porosity produced using -53 fractioned powder, this parameter is even 28 times bigger compared to the dense form (**Koszelow et al. 2021**). In Figure 14, the comparison of the morphology of dense and porous alloys was illustrated. A significantly higher SSA of porous alloy implies a larger possible area of the oxygen-alloy interface, which has a strong influence on the corrosion behaviour of the porous components, as detailed in the following section.

Commented [RL3]: ?

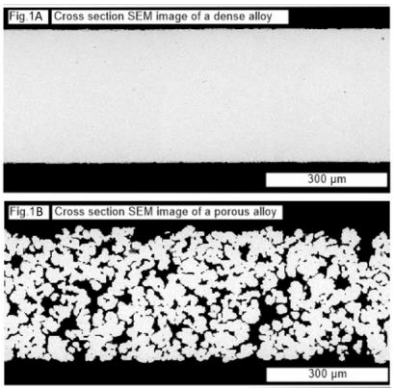

Figure 14. Comparison of Fe22Cr in A) dense and B) porous form.

The most common method of producing the porous alloy sheet is the powder metallurgy. In this technique, the powder is mixed with binders and lubricants and then compressed into the specified shape form. The as-prepared sample is sintered in a protective atmosphere to avoid the oxidation process. Powder metallurgy is widely applied for producing different alloys and composites of metals and ceramics. Furthermore, this method enables the production of a high purity product in a complex shape while controlling its density and porosity (i.e., by adjusting the sintering temperature) (**Rauscher et al. 2008**).

The alternative method to obtain the porous alloy sheet is tape-casting. In this technique, the powder of the desired alloy has to be dispersed in an aqueous or organic medium. Next, binders and plasticisers are added to the mixture to give the tape sufficient strength and flexibility. To prevent big holes and discontinuities within the tape, a defoamer agent is applied or the slurry is degassed. The most important parameter about the slurry is that the powder particles do not drop down by themselves. The as-prepared slurry is cast on the substrate, depending on the used compounds. The most common substrates are metallic foils or special polymer tapes. Then, the tape-casting is performed utilizing the doctor-blade method, which allows for controlling the thickness of the obtained tape. The next step is drying the tape to remove the solvent, and the plastic green tape with connected metallic particles was obtained. In order to remove the binder, the green tape is burned by a thermal treatment at a high enough temperature (usually ~200 – 500 °C) to decompose the binder. The final step is the sintering at reducing conditions to create neck connections between alloy particles and reverse the surface oxidation of the sample, which occurs during the debinding step. The process flow of tape-casting is shown in Figure 2. The final porosity of the as-obtained

sheet depends on the used particle fraction (for larger particle size, the porosity of the final product is larger) and the temperature of reducing sintering. In the case of higher temperatures, the porosity is lower because of grain growth, so the probable pore area is occupied by larger metallic grains (**Rauscher et al. 2008**). Moreover, if the applied temperature is high enough, the full densification occurs, so the tape-casting process can also be used to produce dense metallic sheets.

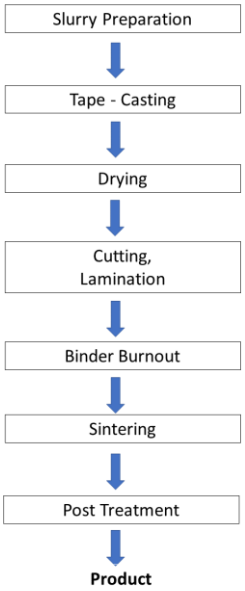

Figure 15. Process flow of tape-casting for the metallic sheet production.

Another technique to obtain porous alloys or metals is the dealloying process. In order to use this method, an alloy that contains the desired elements and one additional element is necessary. For instance, Han et al. (**Han et al. 2020**) obtained pure In and Sn porous metals by the dealloying method. They used pure metal powders to create a pellet by uniaxial pressing. The pellets were then sandwiched with Li foil (molar ratio of Li: In or Li: Sn was 5:1) and sintered at 220–230 °C in a protective Ar atmosphere to form the Li-In or Li-Sn alloy. After alloying, the samples were immersed in dry methanol to extract Li, and a porous foil of In (or Sn) was formed. The schematic diagram of the dealloying process with their corresponding SEM images and XRD patterns of as-obtained products is presented in Figure 3. Dealloying is a more precise process compared with powder metallurgy or tape-casting because it allows for the obtaining of even

nano-porous alloys, which are impossible in the case of other techniques. Mokhtari et al. (**Mokhtari et al. 2020**) obtained the nanoporous FeCr alloy by the dealloying process, so they employed a Fe-Cr-Ni alloy as the precursor. The different compositions of the precursor were immersed for 1 h in a molten Mg bath to obtain the FeCr-Mg structure. Then, highly concentrated nitric acid was applied in order to dissolve the Mg-based solid-state solution, and a FeCr microporous alloy occurred.

Figure 16. Synthesis and characterization of porous metals by chemical dealloying. A) Schematic showing the synthesis of porous In or Sn foil via the dealloying of Li - In or Li – Sn alloy (a Li:In or Li:Sn molar ratio of 5:1 was used). B) SEM image of a dealloyed In sample. C) SEM image of a dealloyed Sn sample. D, E) XRD patterns of D) In and E) Sn samples at different steps of the synthetic procedure (**Han et al. 2020**).

Except for the corrosion process, Cr evaporation from the high chromium alloy limits its application in SOEC systems. These volatile chromium species migrate and deposit on the air electrode, which in turn leads to rapid degradation of the electrochemical performance of the cell. Moreover, chromium evaporation accelerates the corrosion due to decreasing the Cr reservoir, which is a critical factor for the lifespan of the support in MS-SOEC. To prevent this process, protective coatings on the steel interconnects of the SOC stack are generally applied. Such coatings slow down the corrosion process and reduce Cr evaporation.

4. Corrosion properties

4.1 Introduction to high-temperature oxidation

The basic idea behind using metal support in SOCs is to support ceramic element layers with a well-known, low-cost, and robust material, which is expected to lower the cost of SOC devices. Furthermore, alloy support provides thermal strength as well as an electrical connection. However, the oxidation of alloy elements occurs due to the harsh working conditions of HT-SOC devices, which typically operate in the 500-900 °C range. This phenomenon has been observed in ferritic stainless steel alloyed with a high Cr content, which quickly transforms to form a chromia layer. Most metals will inevitably oxidize under a variety of conditions; therefore, the practical challenges of material lifetimes rely on corrosion protection. The strategies revolve around decreasing the oxidation reaction rates, as well as controlling alloy morphology. Controlling the oxidation phenomena requires a fundamental understanding of different aspects of solid-gas reactions. Oxidation rate depends on steel chemistry, temperature and gas atmosphere (**J. Young 2008**).

Therefore, chemical composition and geometrical factor of metal support should be chosen wisely. The surface layer formed by oxidation process dictates the nature of the metal's corrosion rate and has a significant influence on the material. The oxide is protective if it is continuous and efficient in isolating the alloy from the environment. However, if the oxide does not work as a separator, corrosion problems occur. The dense chromium oxide scale decreases the oxidation rate, while accelerated corrosion may lead to support degradation, such as delamination or cracking. Rapid temperature changes cause acceleration of damaging process. In addition, an undesirable chemical reaction between metallic substrate with other cells' elements could be expected. The mechanical state of any solid determines its performance.

The phenomenon of oxidation occurs as a result of the metal reacting with oxygen. In SOC devices, oxygen is acquired from air or steam. Steam, in general, oxidizes quicker than air. Steam-formed oxide layers are more iron-rich and porous, and hence provide less protection. Similarly, air with a high water content accelerates oxidation. The use of certain alloying compounds i.e. Cr, Si and Al improves the resistance to oxidation. Addition of rare earth metals and reactive elements such as Ti, Zr or Y increases oxidation resistance significantly.

Several processes were described, i.e. mass transport through the oxide scale or oxide species evaporation. The considerable role in oxidation process is mechanical stress on the scales and interaction between alloys elements and microstructure. The oxidation rates are typically controlled by diffusion and interfacial mechanisms, where crystallographic and geometrical effects are involved in those processes (**Samal 2016**).

A scheme of oxidation process, resulting in a growing oxide scale is shown in Figure 17 and can be described by following steps: mass transfer in the gas phase causes delivery of oxidant to the gas-scale phase, while the oxygen is incorporated into oxide scale. Meanwhile, oxidized metal from the alloy is transferred into alloy and scale interface, which causes incorporation of metal into scale. As a consequence, metal and/or oxygen transport through the scale is possible.

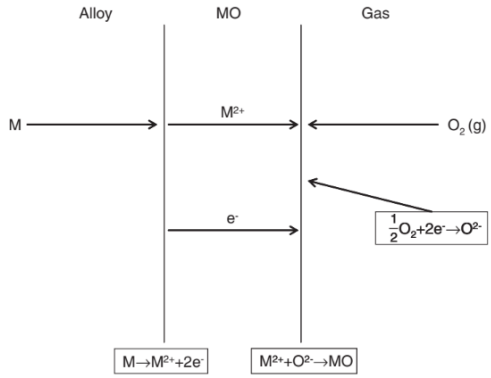

Figure 17. Reactions and transport process involved in growing oxide scale (**J. Young 2008**)

In general, with two metals in the alloy, one of the formed oxides will be more stable than the other oxide. In the most common Fe-Cr alloys, chromium has a greater affinity for oxygen than iron thus, during initial oxidation stage, a thin layer of protective chromia scale is formed. However, exceeding oxidation conditions such as temperature or time, leads to breakaway corrosion. Damaging effect of breakaway corrosion is caused by depletion of chromium in alloy structure as well as formation of iron oxides.

4.2 Oxidation kinetics laws:

The step of reaction is determined by metal consumption, oxygen usage and post-oxidation product formation. Several laws of the kinetics of oxidation are known, i.e. linear wherein surface or interferential process toward the reactive gases is rate controlling and the metal oxidation proceeds at constant rate or logarithmic wherein oxidation process is subjected only for thin oxide scales (2 - 4 nm). In-depth considerations are explained in the second chapter of High-temperature oxidation and corrosion of metals book by Young (**D. J. Young 2016**). In this chapter, parabolic kinetic law is discussed, since it is found that alloys used in MS-SOCs applications obey to. The rate controlling mechanism in parabolic law is the diffusion of metal cations through the oxide scale. This approach started from Wagners' theory, in which the materials corrosion behavior is quantified by parabolic rate constant k_p.

$$\left(\frac{\Delta W}{A}\right)^2 = k_p t,$$

where the ΔW is weight gain, the A is surface area and the t is time. k_p is usually given in g^2m^4s unit. The value of k_p may achieve different values in different temperatures and environments for any material. The target parabolic rate constant for oxidation in green energy devices is $5x10^{-13}$ g^2m^4s.

4.3 Predictive methods – experimental techniques

4.3.1 Oxidation test

For multi-component systems, the requisite thermodynamic, kinetic, and mechanical data are not always available, necessitating further experimental examination. HT-SOCs lifetime should be thousands of hours, therefore, the experimental verification of the predicted results is obligatory before implementation in a real cell.

The oxidation can be investigated by measuring metal or oxygen consumption or by observing oxides growth as a function of time. To predict the lifetime of the alloy, most widely used method is the calculation of oxidation kinetic rates by weight gain measurement, which can be performed by continuous or discontinuous method.

Continuous weight gain measurement

In continuous, thermogravimetry measurement of the alloy sample is attached on the sensitive microbalance, and heated to selected temperature in stable or flowing gas environment. Then, in iso-thermal conditions the weight gain data of alloy sample is collected.

Non-continuous weight gain measurement

In discontinuous method, the samples are placed in the furnace and weighted in interval time of exposition on high-temperature. This method requires a series of samples, subjected to different aging times. The advantage of discontinuous method is the possibility of taken out samples in interval steps. Those samples can be used for post-mortem analysis of range alloys' oxidation stages. From acquired data, the information about the oxidation rate constants and activation energies can be calculated. An exemplary results of the oxidation kinetic tests were proposed by Koszelow et al. and are presented in Figure 18 (**Koszelow et al. 2021**). Recently, Taylor and Tossey have collected and tabulated parabolic rate constants for dozens of alloys by machine learning method and they found that Ni, Cr, Al are the most protective elements. Addition of Mo and Co likewise increase alloys reliability (**Taylor and Tossey 2021**).

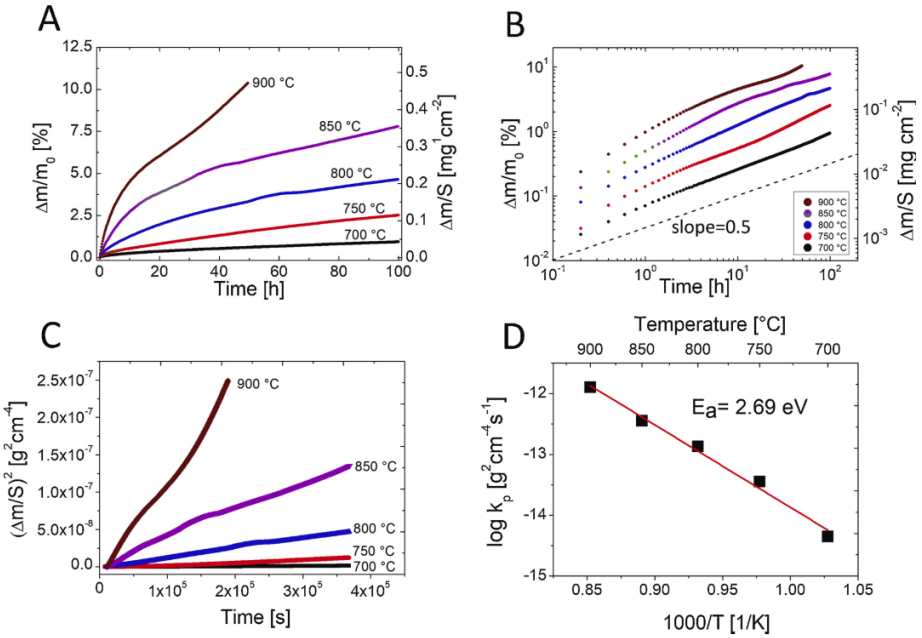

Figure 18. Weight gain data presented as A) linear weight change, B) log-log plot, C) square weight change with respect to the initial surface area and D) Arrhenius plot (**Koszelow et al. 2021**)

4.3.2 Samples examination – post-mortem analysis

Actual changes in the alloy compositional, microstructural and phase constitution information can be observed in post-mortem analyzes.

2D microstructural analysis

Both surface and polished cross-section of the sample morphology could be examined via SEM/EDS analysis. Drewniak et al. (**Drewniak et al. 2021**) proposed accelerated chemical reactivity test by simulating glass-ceramics sealant and metal interconnect interface by using alloy powder. In Figure 19, EDS analysis of their samples before (Figure 19 A) and after (Figure 19 B) aging at 850 °C in static air atmosphere for 500 h is shown. The analysis showed that after aging, a thin layer of chromium oxide had formed on the glass/alloy powder interface and changes in crystallization of the glass matrix.

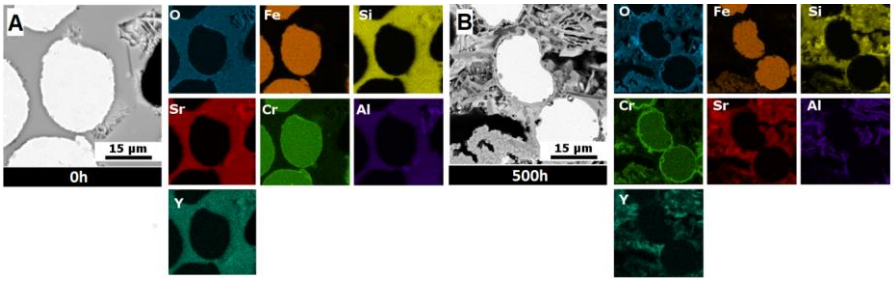

Figure 19. SEM-EDS post-mortem analysis of glass-ceramic and alloy powder interface before (A) and after (B) aging (**Drewniak et al. 2021**)

3D microstructural analysis

In addition to SEM/TEM microscopy, tomographic studies of alloy samples could be performed. Although there are no tomographic studies in the literature of metallic interconnects for SC applications, these studies will be very relevant especially for porous metal supports. Thermographic and tomography analysis will allow the investigation of 3D microstructures of the alloys quantitatively, which strongly supplements the weight gain and microscopic analyses.

Commented [ML5]: I assume there are no tomographic studies in the literature. I am adding a phrase in this sense. If there are any, please add a reference and repharse

Phase identification by XRD

Another complementary method of post-mortem analysis is XRD. Information about the phases (or phase changes) in the investigated alloy can be obtained by matching the resulted diffractogram with tabulated standard. This method allows the identification of post-reaction products. Moreover, XRD measurements can be performed by in-situ mode at the selected temperature.

Chemical state measurements by XPS

XPS analysis can also be used to determine the chemical state of an alloy and its oxides. However, it should be noticed that this method, due to its low penetration, allows only for the surface analysis. Nevertheless, using the XPS technique it is possible to determine the degree of oxidation of the material, so in some cases this approach could be valuable.

Conclusions:

This chapter contributes to the existing knowledge on metallic interconnects and relative corrosion issues, by providing a comprehensive overview of their different roles and systems, processing and deposition methods to assess their functionality in SOEC devices.

Even if it is not possible to unquestionably outline the optimal solution, these findings provide the following insights for coating development:

-The modification of the composition of the base Mn-Co spinel is a promising route to improve the functional properties of the base spinel structure

-A high degree of densification is fundamental to guarantee reasonable protection properties of the coating, in order to limit oxygen inward diffusion to the steel interconnect

- A possible approach to a composite spinel coating (with a proper selection of the powders, formulation of the suspension and post-deposition treatments choice), with the aim of coupling the benefits of rare earth addition with those of Mn-Co spinel, might be explored.

The preliminary findings on the role of the porous metal alloys support show that the MS-SOEC design has promises, but further work and recommendations are required to properly evaluate the MS feasibility. Continued development of MS-SOEC will be beneficial if performance, durability, or cost can be enhanced beyond that of other SOEC types. The best candidate for SOC applications seems to be chromia forming ferritic alloys. At SOC operating conditions, these alloys passivate, providing sufficient electrical conductivity and corrosion resistance. The porous forms of the alloys are also promising, however the corrosion process of them has to be researched in detail. It is found that Ni, Crand Al are the most corrosion protective elements. To prevent chromium evaporation and poisoning the electrodes, the functional coatings, for instance Mn-Co spinel, are applied to the steel components. Theoretical bases for predictive methodologies include compositional, microstructure and phase changes. Wagner's kinetic model is the most common approach to predict high-temperature oxidation resistance. However, parabolic rate constants may hinder a multiplicity of processes in addiction to mass gain. For a better understanding of high-temperature corrosion effects in metal supports, both kinetic and further structural investigations are necessary.

REFERENCES:

Aznam, Isyraf, Joelle C.W. Mah, Andanastuti Muchtar, Mahendra R. Somalu, and Mariyam J. Ghazali. 2021. 'Electrophoretic deposition of (Cu,Mn,Co)3O4 spinel coating on SUS430 ferritic

stainless steel: Process and performance evaluation for solid oxide fuel cell interconnect applications', *Journal of the European Ceramic Society*, 41. Elsevier Ltd: 1360–1373.

Belogolovsky, I., X.-D. Zhou, H. Kurokawa, P. Y. Hou, S. Visco, and H. U. Anderson. 2007. 'Effects of Surface-Deposited Nanocrystalline Chromite Thin Films on the Performance of a Ferritic Interconnect Alloy', *Journal of The Electrochemical Society*, 154: B976.

Bianco, Manuel, Jan Pieter Ouweltjes, and Jan Van herle. 2019. 'Degradation analysis of commercial interconnect materials for solid oxide fuel cells in stacks operated up to 18000 hours', *International Journal of Hydrogen Energy*, 44. Elsevier Ltd: 31406–31422.

Bianco, Manuel, Stephane Poitel, Jong-Eun Hong, Shicai Yang, Zhu-Jun Wang, Marc Willinger, Robert Steinberger-Wilckens, and Jan Van herle. 2020. 'Corrosion behaviour of nitrided ferritic stainless steels for use in solid oxide fuel cell devices', *Corrosion Science*, 165: 108414.

Blum, Ludger, Qingping Fang, Sonja M. Groß-Barsnick, L. G.J.(Bert) de Haart, Jürgen Malzbender, Norbert H. Menzler, and Willem J. Quadakkers. 2020. 'Long-term operation of solid oxide fuel cells and preliminary findings on accelerated testing', *International Journal of Hydrogen Energy*,: 1–10.

Bobruk, M., S. Molin, M. Chen, T. Brylewski, and P.V. Hendriksen. 2018. 'Sintering of MnCo2O4 coatings prepared by electrophoretic deposition', *Materials Letters*, 213. Elsevier B.V.: 394–398.

Brylewski, T., W. Kucza, A. Adamczyk, A. Kruk, M. Stygar, M. Bobruk, and J. Dąbrowa. 2014. 'Microstructure and electrical properties of Mn1+xCo2−xO4 (0≤x≤1.5) spinels synthesized using EDTA-gel processes', *Ceramics International*, 40: 13873–13882.

Brylewski, T., S. Molin, M. Marczyński, Mazur, K. Domaradzki, O. Kryshtal, and A. Gil. 2021. 'Influence of Gd deposition on the oxidation behavior and electrical properties of a layered system consisting of Crofer 22 APU and MnCo2O4 spinel', *International Journal of Hydrogen Energy*, 46: 6775–6791.

Chen, Guoyi, Xianshuang Xin, Ting Luo, Leimin Liu, Yuchun Zhou, Chun Yuan, Chucheng Lin, Zhongliang Zhan, and Shaorong Wang. 2015. 'Mn1.4Co1.4Cu0.2O4 spinel protective coating on ferritic stainless steels for solid oxide fuel cell interconnect applications', *Journal of Power Sources*, 278. Elsevier B.V: 230–234.

Chesson, D. A., and J. H. Zhu. 2020. 'Effect of Off-Stoichiometry on Electrical Conductivity in Ni-Fe and Mn-Co Spinel Systems', *Journal of The Electrochemical Society*, 167. IOP Publishing: 124515.

Chevalier, S., and J. P. Larpin. 2002. 'Formation of perovskite type phases during the high temperature oxidation of stainless steels coated with reactive element oxides', *Acta Materialia*, 50: 3107–3116.

Chu, Chun Lin, Jye Lee, Tien Hsi Lee, and Yung Neng Cheng. 2009. 'Oxidation behavior of metallic interconnect coated with La-Sr-Mn film by screen painting and plasma sputtering', *International Journal of Hydrogen Energy*, 34. International Association for Hydrogen Energy: 422–434.

Drewniak, A., D. Koszelow, P. Błaszczak, K. Górnicka, K. Jurak, H. Javed, A. G. Sabato, P. Jasiński, S. Molin, and F. Smeacetto. 2021. 'Glass-ceramic sealants and steel interconnects: Accelerated interfacial stability and reactivity tests at high temperature', *Materials and Design*, 212.

Falk-Windisch, Hannes, Julien Claquesin, Mohammad Sattari, Jan-Erik Svensson, and Jan Froitzheim. 2017. 'Co- and Ce/Co-coated ferritic stainless steel as interconnect material for Intermediate Temperature Solid Oxide Fuel Cells', *Journal of Power Sources*, 343: 1–10.

Fontana, S., R. Amendola, S. Chevalier, P. Piccardo, G. Caboche, M. Viviani, R. Molins, and M. Sennour. 2007. 'Metallic interconnects for SOFC: Characterisation of corrosion resistance and conductivity evaluation at operating temperature of differently coated alloys', *Journal of Power Sources*, 171: 652–662.

Fontana, S., S. Chevalier, and G. Caboche. 2012. 'Metallic Interconnects for Solid Oxide Fuel Cell: Performance of Reactive Element Oxide Coating During 10, 20 and 30 Months Exposure', *Oxidation of Metals*, 78: 307–328.

Gambino, L. V., N. J. Magdefrau, and M. Aindow. 2015. 'Microstructural effects of the reduction step in reactive consolidation of manganese cobaltite coatings on Crofer 22 APU', *Materials at High Temperatures*, 32: 142–147.

Goebel, Claudia, Vijayshankar Asokan, Sarah Khieu, Jan Erik Svensson, and Jan Froitzheim. 2021. 'Self-healing properties of Ce/Co-coated stainless steel under simulated intermediate temperature solid oxide fuel cell conditions', *Surface and Coatings Technology*, 428. Elsevier B.V.: 127894.

Goebel, Claudia, Robert Berger, Carlos Bernuy-Lopez, Jörgen Westlinder, Jan Erik Svensson, and Jan Froitzheim. 2020. 'Long-term (4 year) degradation behavior of coated stainless steel 441 used for solid oxide fuel cell interconnect applications', *Journal of Power Sources*, 449.

Goebel, Claudia, Alexander G. Fefekos, Jan Erik Svensson, and Jan Froitzheim. 2018. 'Does the conductivity of interconnect coatings matter for solid oxide fuel cell applications?', *Journal of*

Power Sources, 383. Elsevier: 110–114.

Guo, P Y, H Sun, Y Shao, J T Ding, J C Li, M R Huang, S Y Mao, et al. 2020. 'The evolution of microstructure and electrical performance in doped Mn-Co and Cu-Mn oxide layers with the extended oxidation time', *Corrosion Science*, 172.

Guo, Pingyi, Yongbiao Lai, Yong Shao, Yu Zhang, Hang Sun, and Yuxin Wang. 2018. 'Oxidation characteristics and electrical properties of doped Mn-Co spinel reaction layer for solid oxide fuel cell metal interconnects', *Coatings*, 8.

Hamaker, H. C. 1940. 'Formation of a deposit by electrophoresis', *Transactions of the Faraday Society*, 35: 279.

Han, Sang Yun, John A. Lewis, Pralav P. Shetty, Jared Tippens, David Yeh, Thomas S. Marchese, and Matthew T. McDowell. 2020. 'Porous Metals from Chemical Dealloying for Solid-State Battery Anodes', *Chemistry of Materials*, 32: 2461–2469.

Hassan, Muhammad Aqib, Othman Bin Mamat, and Muhammad Mehdi. 2020. 'Review: Influence of alloy addition and spinel coatings on Cr-based metallic interconnects of solid oxide fuel cells', *International Journal of Hydrogen Energy*, 45. Elsevier Ltd: 25191–25209.

Holt, Arve, and Per Kofstad. 1994. 'Electrical conductivity and defect structure of Cr2O3. II. Reduced temperatures (<∼1000°C)', *Solid State Ionics*, 69: 137–143.

Hosseini, N., M.H. Abbasi, F. Karimzadeh, and G.M. Choi. 2015. 'Development of Cu1.3Mn1.7O4 spinel coating on ferritic stainless steel for solid oxide fuel cell interconnects', *Journal of Power Sources*, 273. Elsevier B.V: 1073–1083.

Hou, P. Y., and J. Stringer. 1995. 'The effect of reactive element additions on the selective oxidation, growth and adhesion of chromia scales', *Materials Science and Engineering A*, 202: 1–10.

Hou, P.Y. 2000. 'Sulfur segregation to growing Al2O3/alloy interfaces', *Journal of Materials Science Letters*, 19: 577–578.

Ignaczak, Justyna, Yevgeniy Naumovich, Karolina Górnicka, Jan Jamroz, Wojciech Wróbel, Jakub Karczewski, Ming Chen, Piotr Jasiński, and Sebastian Molin. 2020. 'Preparation and characterisation of iron substituted Mn1.7Cu1.3-xFexO4 spinel oxides (x = 0, 0.1, 0.3, 0.5)', *Journal of the European Ceramic Society*, 40: 5920–5929.

Javed, Hassan, Theo Saunders, Michael John Reece, Elisa Zanchi, Antonio Gianfranco Sabato, Aldo R. Boccaccini, and Federico Smeacetto. 2021. 'Pressure assisted flash sintering of Mn-Co based spinel coatings for solid oxide electrolysis cells (SOECs)', *Ceramics International*, 47:

17804–17808.

Jeong, H., D. Roehrens, and M. Bram. 2020. 'Facile route for reactive coating of LaCrO3 on high-chromium steels as protective layer for solid oxide fuel cell applications', *Materials Letters*, 258. Elsevier B.V.: 126794.

Johnson, Christopher, Randall Gemmen, and Nina Orlovskaya. 2004. 'Nano-structured self-assembled LaCrO3 thin film deposited by RF-magnetron sputtering on a stainless steel interconnect material', *Composites Part B: Engineering*, 35: 167–172.

Kalinina, Elena, and Elena Pikalova. 2021. 'Opportunities, challenges and prospects for electrodeposition of thin-film functional layers in solid oxide fuel cell technology', *Materials*, 14.

Koszelow, D., M. Makowska, F. Marone, J. Karczewski, P. Jasiński, and S. Molin. 2021. 'High temperature corrosion evaluation and lifetime prediction of porous Fe22Cr stainless steel in air in temperature range 700–900 °C', *Corrosion Science*, 189.

Lee, Kunho, Byoungyoung Yoon, Juhyun Kang, Sanghun Lee, and Joongmyeon Bae. 2017. 'Evaluation of Ag-doped (MnCo)3O4 spinel as a solid oxide fuel cell metallic interconnect coating material', *International Journal of Hydrogen Energy*, 42. Elsevier Ltd: 29511–29517.

Lee, Shyong, Chun Lin Chu, Ming Jui Tsai, and Jye Lee. 2010. 'High temperature oxidation behavior of interconnect coated with LSCF and LSM for solid oxide fuel cell by screen printing', *Applied Surface Science*, 256: 1817–1824.

Li, Jun, Chunyan Xiong, Jin Li, Dong Yan, Jian Pu, Bo Chi, and Li Jian. 2017. 'Investigation of MnCu0.5Co1.5O4 spinel coated SUS430 interconnect alloy for preventing chromium vaporization in intermediate temperature solid oxide fuel cell', *International Journal of Hydrogen Energy*, 42. Elsevier Ltd: 16752–16759.

Liu, Y., Jeffrey W. Fergus, K. Wang, and C. Dela Cruz. 2013. 'Crystal Structure, Chemical Stabilities and Electrical Conductivity of Fe-Doped Manganese Cobalt Spinel Oxides for SOFC Interconnect Coatings', *Journal of the Electrochemical Society*, 160: F1316–F1321.

Magdefrau, Neal J., Lei Chen, Ellen Y. Sun, Jean Yamanis, and Mark Aindow. 2013. 'Formation of spinel reaction layers in manganese cobaltite-coated Crofer22 APU for solid oxide fuel cell interconnects', *Journal of Power Sources*, 227. Elsevier B.V: 318–326.

Magrasó, Anna, Hannes Falk-Windisch, Jan Froitzheim, Jan Erik Svensson, and Reidar Haugsrud. 2015. 'Reduced long term electrical resistance in Ce/Co-coated ferritic stainless steel for solid oxide fuel cell metallic interconnects', *International Journal of Hydrogen Energy*, 40: 8579–

8585.

Mah, Joelle C.W., Andanastuti Muchtar, Mahendra R. Somalu, and Mariyam J. Ghazali. 2017. 'Metallic interconnects for solid oxide fuel cell: A review on protective coating and deposition techniques', *International Journal of Hydrogen Energy*, 42: 9219–9229.

Mah, Joelle C.W., Andanastuti Muchtar, Mahendra R. Somalu, Mariyam J. Ghazali, and Jarot Raharjo. 2017. 'Formation of sol–gel derived (Cu,Mn,Co)3O4 spinel and its electrical properties', *Ceramics International*, 43. Elsevier Ltd: 7641–7646.

Masi, Andrea, Mariangela Bellusci, Stephen J. McPhail, Franco Padella, Priscilla Reale, Jong-Eun Hong, Robert Steinberger-Wilckens, and Maurizio Carlini. 2016. 'The effect of chemical composition on high temperature behaviour of Fe and Cu doped Mn-Co spinels', *Ceramics International*, 43: 2829–2835.

Masi, Andrea, Mariangela Bellusci, Stephen J. McPhail, Franco Padella, Priscilla Reale, Jong Eun Hong, Robert Steinberger-Wilckens, and Maurizio Carlini. 2017. 'Cu-Mn-Co oxides as protective materials in SOFC technology: The effect of chemical composition on mechanochemical synthesis, sintering behaviour, thermal expansion and electrical conductivity', *Journal of the European Ceramic Society*, 37. Elsevier Ltd: 661–669.

Menzler, Norbert H., Doris Sebold, and Olivier Guillon. 2018. 'Post-test characterization of a solid oxide fuel cell stack operated for more than 30,000 hours: The cell', *Journal of Power Sources*, 374. Elsevier: 69–76.

Mokhtari, Morgane, Takeshi Wada, Christophe Le Bourlot, Jannick Duchet-Rumeau, Hidemi Kato, Eric Maire, and Nicolas Mary. 2020. 'Corrosion resistance of porous ferritic stainless steel produced by liquid metal dealloying of Incoloy 800', *Corrosion Science*, 166. Elsevier: 108468.

Molin, S., P. Jasinski, L. Mikkelsen, W. Zhang, M. Chen, and P. V. Hendriksen. 2016. 'Low temperature processed MnCo2O4and MnCo1.8Fe0.2O4 as effective protective coatings for solid oxide fuel cell interconnects at 750 °C', *Journal of Power Sources*, 336. Elsevier B.V: 408–418.

Molin, S., A. G. Sabato, M. Bindi, P. Leone, G. Cempura, M. Salvo, S. Cabanas Polo, A. R. Boccaccini, and F. Smeacetto. 2017. 'Microstructural and electrical characterization of Mn-Co spinel protective coatings for solid oxide cell interconnects', *Journal of the European Ceramic Society*, 37. Elsevier Ltd: 4781–4791.

Molin, S., A.G. Sabato, H. Javed, G. Cempura, A.R. Boccaccini, and F. Smeacetto. 2018. 'Co-deposition of CuO and Mn1.5Co1.5O4 powders on Crofer22APU by electrophoretic method:

Structural, compositional modifications and corrosion properties', *Materials Letters*, 218. Elsevier B.V.: 329–333.

Mosavi, Ali, and Hadi Ebrahimifar. 2020. 'Investigation of oxidation and electrical behavior of AISI 430 steel coated with Mn–Co–CeO2 composite', *International Journal of Hydrogen Energy*, 45. Elsevier Ltd: 3145–3162.

Paknahad, Pouyan, Masoud Askari, and Milad Ghorbanzadeh. 2014. 'Application of sol-gel technique to synthesis of copper-cobalt spinel on the ferritic stainless steel used for solid oxide fuel cell interconnects', *Journal of Power Sources*, 266. Elsevier Ltd: 79–87.

Pan, Yue, Shujiang Geng, Gang Chen, and Fuhui Wang. 2021a. 'CuFe2O4/CuO coating for solid oxide fuel cell steel interconnects', *International Journal of Hydrogen Energy*, 46. Elsevier Ltd: 22942–22955.

Pan, Yue, Shujiang Geng, Gang Chen, and Fuhui Wang. 2021b. 'Thermal conversion process of CuFe2O4 coating on steel interconnect for solid oxide fuel cell applications', *Materials Letters*, 297. Elsevier B.V.: 129967.

Pandiyan, Sathish, Ahmad El-Kharouf, and Robert Steinberger-Wilckens. 2020. 'Formulation of spinel based inkjet inks for protective layer coatings in SOFC interconnects', *Journal of Colloid and Interface Science*, 579. Elsevier Inc.: 82–95.

Park, Beom Kyeong, Jong Won Lee, Seung Bok Lee, Tak Hyoung Lim, Seok Joo Park, Chong Ook Park, and Rak Hyun Song. 2013. 'Cu- and Ni-doped Mn1.5Co1.5O4 spinel coatings on metallic interconnects for solid oxide fuel cells', *International Journal of Hydrogen Energy*, 38. Elsevier Ltd: 12043–12050.

Park, Mansoo, Ji Su Shin, Sanghyeok Lee, Hyo Jin Kim, Hyegsoon An, Ho il Ji, Hyoungchul Kim, et al. 2018. 'Thermal degradation mechanism of ferritic alloy (Crofer 22 APU)', *Corrosion Science*, 134: 17–22.

Persson, Å.H., L. Mikkelsen, P.V. Hendriksen, and M.A.J. Somers. 2012. 'Interaction mechanisms between slurry coatings and solid oxide fuel cell interconnect alloys during high temperature oxidation', *Journal of Alloys and Compounds*, 521: 16–29.

Piccardo, P., P. Gannon, S. Chevalier, M. Viviani, A. Barbucci, G. Caboche, R. Amendola, and S. Fontana. 2007. 'ASR evaluation of different kinds of coatings on a ferritic stainless steel as SOFC interconnects', *Surface and Coatings Technology*, 202: 1221–1225.

Puranen, Jouni, Mikko Pihlatie, Juha Lagerbom, Giovanni Bolelli, Jarmo Laakso, Leo Hyvärinen, Mikko Kylmälahti, et al. 2014. 'Post-mortem evaluation of oxidized atmospheric plasma

sprayed Mn-Co-Fe oxide spinel coatings on SOFC interconnectors', *International Journal of Hydrogen Energy*, 39: 17284–17294.

Pyo, Seong Soo, Seung Bok Lee, Tak Hyoung Lim, Rak Hyun Song, Dong Ryul Shin, Sang Hoon Hyun, and Young Sung Yoo. 2011. 'Characteristic of (La0.8Sr0.2)0.98MnO 3 coating on Crofer22APU used as metallic interconnects for solid oxide fuel cell', *International Journal of Hydrogen Energy*, 36. Elsevier Ltd: 1868–1881.

Qi, H B, and D G Lees. 2000. 'The Effects of Surface-Applied Oxide Films Containing Varying Amounts of Yttria , Chromia , or Alumina on the High-Temperature Oxidation Behavior of Chromia-Forming and Alumina-Forming Alloys', *Oxidation of Metals*, 53: 507–527.

Qu, Wei, Jian Li, and Douglas G. Ivey. 2004. 'Sol-gel coatings to reduce oxide growth in interconnects used for solid oxide fuel cells', *Journal of Power Sources*, 138: 162–173.

Quadakkers, W.J., J. Piron-Abellan, V. Shemet, and L. Singheiser. 2003. 'Metallic interconnectors for solid oxide fuel cells – a review', *Materials at High Temperatures*, 20: 115–127.

Rauscher, Martin, Georg Besendörfer, and Andreas Roosen. 2008. 'Steel-sheet fabrication by tape casting', *International Journal of Powder Metallurgy (Princeton, New Jersey)*, 44: 39–48.

Sabato, A.G., S. Molin, H. Javed, E. Zanchi, A.R. Boccaccini, and F. Smeacetto. 2019. 'In-situ Cu-doped MnCo-spinel coatings for solid oxide cell interconnects processed by electrophoretic deposition', *Ceramics International*, 45. Techna Group S.r.l.: 19148–19157.

Sabato, A.G., E. Zanchi, S. Molin, G. Cempura, H. Javed, K. Herbrig, C. Walter, A.R. Boccaccini, and F. Smeacetto. 2021. 'Mn-Co spinel coatings on Crofer 22 APU by electrophoretic deposition: Up scaling, performance in SOFC stack at 850 °C and compositional modifications', *Journal of the European Ceramic Society*, 41. Elsevier Ltd: 4496–4504.

Samal, Sneha. 2016. 'High-temperature oxidation of metals', In *High-temperature corrosion*, 11–17.

Seo, Hyung Suk, Guangxi Jin, Jae Ho Jun, Do Hyeong Kim, and Kyoo Young Kim. 2008. 'Effect of reactive elements on oxidation behaviour of Fe-22Cr-0.5Mn ferritic stainless steel for a solid oxide fuel cell interconnect', *Journal of Power Sources*, 178: 1–8.

Shaigan, Nima, Douglas G. Ivey, and Weixing Chen. 2008. 'Co/LaCrO3 composite coatings for AISI 430 stainless steel solid oxide fuel cell interconnects', *Journal of Power Sources*, 185: 331–337.

Shaigan, Nima, Wei Qu, Douglas G. Ivey, and Weixing Chen. 2010. 'A review of recent progress in coatings, surface modifications and alloy developments for solid oxide fuel cell ferritic

stainless steel interconnects', *Journal of Power Sources*, 195: 1529–1542.

Smeacetto, Federico, Auristela De Miranda, Sandra Cabanas Polo, Sebastian Molin, Dino Boccaccini, Milena Salvo, and Aldo R. Boccaccini. 2015. 'Electrophoretic deposition of Mn1.5Co1.5O4 on metallic interconnect and interaction with glass-ceramic sealant for solid oxide fuel cells application', *Journal of Power Sources*, 280. Elsevier B.V: 379–386.

Spotorno, R, P Piccardo, F Perrozzi, S Valente, M Viviani, and A Ansar. 2015. 'Microstructural and Electrical Characterization of Plasma Sprayed Cu-Mn Oxide Spinels as Coating on Metallic Interconnects for Stacking Solid Oxide Fuel Cells ~': 728–734.

Steele, Brian C.H., and Angelika Heinzel. 2001. 'Materials for fuel-cell technologies', *Nature*, 414: 345–352.

Stevenson, J. W., Z. G. Yang, G. G. Xia, Z. Nie, and J. D. Templeton. 2013. 'Long-term oxidation behavior of spinel-coated ferritic stainless steel for solid oxide fuel cell interconnect applications', *Journal of Power Sources*, 231. Elsevier B.V: 256–263.

Sun, Zhihao, Ruofan Wang, Alexey Y. Nikiforov, Srikanth Gopalan, Uday B. Pal, and Soumendra N. Basu. 2018. 'CuMn1.8O4 protective coatings on metallic interconnects for prevention of Cr-poisoning in solid oxide fuel cells', *Journal of Power Sources*, 378. Elsevier: 125–133.

Talic, Belma, Peter Vang Hendriksen, Kjell Wiik, and Hilde Lea Lein. 2018. 'Thermal expansion and electrical conductivity of Fe and Cu doped MnCo2O4spinel', *Solid State Ionics*, 326. Elsevier: 90–99.

Talic, Belma, Peter Vang Hendriksen, Kjell Wiik, and Hilde Lea Lein. 2019. 'Diffusion couple study of the interaction between Cr 2 O 3 and MnCo 2 O 4 doped with Fe and Cu', *Solid State Ionics*, 332. Elsevier: 16–24.

Talic, Belma, Sebastian Molin, Peter Vang Hendriksen, and Hilde Lea Lein. 2018. 'Effect of pre-oxidation on the oxidation resistance of Crofer 22 APU', *Corrosion Science*, 138: 189–199.

Talic, Belma, Sebastian Molin, Kjell Wiik, Peter Vang Hendriksen, and Hilde Lea Lein. 2017. 'Comparison of iron and copper doped manganese cobalt spinel oxides as protective coatings for solid oxide fuel cell interconnects', *Journal of Power Sources*, 372. Elsevier: 145–156.

Tan, K. H., H. A. Rahman, and H. Taib. 2019. 'Coating layer and influence of transition metal for ferritic stainless steel interconnector solid oxide fuel cell: A review', *International Journal of Hydrogen Energy*, 44. Elsevier Ltd: 30591–30605.

Taylor, Christopher D., and Brett M. Tossey. 2021. 'High temperature oxidation of corrosion resistant alloys from machine learning', *npj Materials Degradation*, 5. Springer US: 1–10.

Thaheem, Imdadullah, Dong Woo Joh, Taimin Noh, Ha-ni Im, and Kang Taek Lee. 2021. 'Physico-electrochemical properties and long-term stability of Mn1.45-0.5xCo1.45-0.5xCuxY0.1O4 spinel protective coatings on commercial metallic interconnects for solid oxide fuel cells', *Journal of Industrial and Engineering Chemistry*, 96: 315–321.

Thyssenkrupp. 2001a. 'AISI430 Material Data Sheet'.

Thyssenkrupp. 2001b. 'AISI441 Material Data Sheet'.

ThyssenKrupp VDM GmbH. 2012. 'CROFER 22 H: Oxidation-Resistant Ferritic Stainless Steel', *Alloy Digest*,.

Tsai, Ming Jui, Chun Lin Chu, and Shyong Lee. 2010. 'La0.6Sr0.4Co0.2Fe0.8O3 protective coatings for solid oxide fuel cell interconnect deposited by screen printing', *Journal of Alloys and Compounds*, 489: 576–581.

Tseng, Hui Ping, Tung Yuan Yung, Chien Kuo Liu, Yung Neng Cheng, and Ruey Yi Lee. 2020. 'Oxidation characteristics and electrical properties of La- or Ce-doped MnCo2O4 as protective layer on SUS441 for metallic interconnects in solid oxide fuel cells', *International Journal of Hydrogen Energy*, 45. Elsevier Ltd: 12555–12564.

Tucker, Michael C. 2020. 'Progress in metal-supported solid oxide electrolysis cells: A review', *International Journal of Hydrogen Energy*,. Elsevier Ltd.

VDM-Metals. 2010. 'Crofer 22 APU Material Data Sheet'.

Waluyo, Nurhadi S., Beom Kyeong Park, Seung Bok Lee, Tak Hyoung Lim, Seok Joo Park, Rak Hyun Song, and Jong Won Lee. 2014. '(Mn,Cu)3O4-based conductive coatings as effective barriers to high-temperature oxidation of metallic interconnects for solid oxide fuel cells', *Journal of Solid State Electrochemistry*, 18: 445–452.

Wang, Ruofan, Zhihao Sun, Uday B. Pal, Srikanth Gopalan, and Soumendra N. Basu. 2018. 'Mitigation of chromium poisoning of cathodes in solid oxide fuel cells employing CuMn1.8O4 spinel coating on metallic interconnect', *Journal of Power Sources*, 376. Elsevier: 100–110.

Xiao, Jinhua, Wenying Zhang, Chunyan Xiong, Bo Chi, Jian Pu, and Li Jian. 2016. 'Oxidation behavior of Cu-doped MnCo2O4 spinel coating on ferritic stainless steels for solid oxide fuel cell interconnects', *International Journal of Hydrogen Energy*, 41: 9611–9618.

Xin, Xianshuang, Shaorong Wang, Jiqin Qian, Chucheng Lin, and Zhongliang Zhan. 2011. 'Development of the spinel powder reduction technique for solid oxide fuel cell interconnect coating', *International Journal of Hydrogen Energy*, 37. Elsevier Ltd: 471–476.

You, Peng Fei, Xue Zhang, Hai Liang Zhang, and Chao Liu Zeng. 2018. 'Oxidation Behavior of

NiFe2O4 Spinel-Coated Interconnects in Wet Air', *Oxidation of Metals*, 90. Springer US: 499–513.

You, Pengfei, Xue Zhang, Hailiang Zhang, Xiaoguang Yang, and Chaoliu Zeng. 2020. 'Effect of Nb Additions on the High-Temperature Performances of NiFe2O4 Spinel Coatings Fabricated on Ferritic Stainless Steel', *Oxidation of Metals*, 93. Springer US: 465–482.

Young, David J. 2016. 'Enabling Theory', *High Temperature Oxidation and Corrosion of Metals*,: 31–84.

Young, John. 2008. 'Chapter 1 The Nature of High Temperature Oxidation', *Corrosion Series*, 1: 1–27.

Zanchi, E., A.G. Sabato, S. Molin, G. Cempura, A.R. Boccaccini, and F. Smeacetto. 2021. 'Recent advances on spinel-based protective coatings for solid oxide cell metallic interconnects produced by electrophoretic deposition', *Materials Letters*, 286: 129229.

Zanchi, E., B. Talic, A.G. Sabato, S. Molin, A.R. Boccaccini, and F. Smeacetto. 2019. 'Electrophoretic co-deposition of Fe2O3 and Mn1,5Co1,5O4: Processing and oxidation performance of Fe-doped Mn-Co coatings for solid oxide cell interconnects', *Journal of the European Ceramic Society*, 39. Elsevier: 3768–3777.

Zanchi, E, S Molin, A.G. Sabato, B Talic, G Cempura, A.R. Boccaccini, and F Smeacetto. 2020. 'Iron doped manganese cobaltite spinel coatings produced by electrophoretic co-deposition on interconnects for solid oxide cells: Microstructural and electrical characterization', *Journal of Power Sources*, 455. Elsevier B.V.: 227910.

Zhu, J. H., D. A. Chesson, and Y. T. Yu. 2021. 'Review—(Mn,Co) 3 O 4 -Based Spinels for SOFC Interconnect Coating Application', *Journal of The Electrochemical Society*, 168: 114519.

Zhu, J. H., Y. Zhang, A. Basu, Z. G. Lu, M. Paranthaman, D. F. Lee, and E. A. Payzant. 2004. 'LaCrO3-based coatings on ferritic stainless steel for solid oxide fuel cell interconnect applications', *Surface and Coatings Technology*, 177–178: 65–72.

Zhu, J H, M J Lewis, S W Du, and Y T Li. 2015. 'CeO2-doped (Co, Mn)3O4 coatings for protecting solid oxide fuel cell interconnect alloys', *Thin Solid Films*, 596: 179–184.